Downloaded from rsta.royalsocietypublishing.org

PHILOSOPHICAL TRANSACTIONS OF THE ROYAL SOCIETY A MATHEMATICAL, PHYSICAL & ENGINEERING SCIENCES

# Pulsars as Probes of Newtonian Dynamical Systems

E. S. Phinney

*Phil. Trans. R. Soc. Lond. A* 1992 **341**, 39-75
doi: 10.1098/rsta.1992.0084

**Email alerting service**

Receive free email alerts when new articles cite this article - sign up in the box at the top right-hand corner of the article or click **here**

To subscribe to *Phil. Trans. R. Soc. Lond. A* go to:
**http://rsta.royalsocietypublishing.org/subscriptions**

This journal is © 1992 The Royal Society

Downloaded from rsta.royalsocietypublishing.org

# Pulsars as probes of newtonian dynamical systems

By E. S. Phinney

*Theoretical Astrophysics, 151-33 Caltech, Pasadena, California 91125, U.S.A.*

As clocks, pulsars rival the best atomic clocks on Earth. Though the rest-frame 'tick' rate (period $P$) of any given pulsar is unknown, the rest-frame rates of change of the periods are known to be very small. Therefore when they are observed to be large, one is quite certain that the rate of changes must be due to changing Doppler shifts: $\dot{P}$ to acceleration, $\ddot{P}$ to jerk, and periodic shifts to orbiting companion stars or planets. The first two give otherwise unobtainable information on the density and masses of the stellar remnants in the cores of globular clusters. The orbits of binary pulsars provide a test of the theory of the evolution of red giant stars, and in globular clusters provide the first direct evidence for the three- and four-body encounters which are believed to determine the dynamical evolution of globular clusters. The orbits of binary pulsars in our own Galaxy also show evidence for the fluctuations which the fluctuation–dissipation theorem implies should occur during the dissipative tidal circularization of orbits. And newtonian dynamical effects may soon add irrefutable confirmation to recent observations suggesting that some pulsars are surrounded by planetary systems similar to our own. There may not be life on their planets, but pulsars certainly breathe new life into the study of newtonian dynamical systems.

## 1. Introduction

Except for some small effects, such as the precession of the perihelia of the inner planets and gas outflows from comets, the dynamics of the solar system is described with extraordinary accuracy by the simple laws of newtonian dynamics. The current high precision of Solar System ephemerides come largely from measurements of the light-travel time of signals between the Earth and local oscillators on spacecraft (both free-flying and on the surfaces of moons and planets). A pulsar orbiting another body is a similarly precisely predictable clock. If the pulsar in its orbit moves farther from the Earth, the arrival times of its pulses will be delayed by the time it takes light to traverse the increased distance. (This effect was discovered in 1675 by the Danish astronomer Ole Roemer, who noticed that the times of eclipses of Jupiter's satellites varied periodically over the year by $\pm 8$ min. He correctly attributed this variation to the time it took light to cross the Earth's orbit. Pulsar astronomers still worry about making this correction for the Earth's motion, to ensure that changes in the pulse arrival times are due to the pulsar alone, and not to uncorrected parts of the Earth's motion!)

The most accurate measurements of pulse arrival time, and hence change in pulsar distance, require a pulsar with a short spin period, a stable pulse profile, and a stable spin rate. Conveniently, nature has arranged to put pulsars with these properties

*Phil. Trans. R. Soc. Lond.* A (1992) **341**, 39–75
*Printed in Great Britain*

© 1992 The Royal Society



The Royal Society is collaborating with JSTOR to digitize, preserve, and extend access to *Philosophical Transactions: Physical Sciences and Engineering.* www.jstor.org

Downloaded from rsta.royalsocietypublishing.org



exactly in those environments where the distance measurements they allow are the most interesting! This may be because the stablest pulsars are old ones whose apparently weak magnetic fields put small stresses on their neutron star crusts. For such a neutron star to have acquired a short period, it must have acquired angular momentum by accreting matter from a companion star. Since a neutron star must typically wait a long time after its formation for a companion star to come close enough (or swell up enough) for the neutron star to pull mass off it, neutron stars which have accreted matter are generally old and stable. So pulsars in binary systems (or in globular clusters, where the density of stars is high enough that binaries can be disrupted by passing stars) tend to be the ones which can be timed very precisely. Timing residuals of $10^1$–$10^2$ μs per observation are not uncommon. For periodic terms, observations over many orbits can be averaged, improving the accuracy in the mean by the square root of the number of orbits averaged. In many binary pulsars, the averaged residuals are $\sim 1$ μs, so the pulsar's changing distance from Earth is known to a precision of $\sim c(1\ \mu\text{s}) = 300$ m. Since this is a small fraction of a neutron's star's $\sim 10$ km radius, one might worry that residuals of this order might be caused by changes in the pulsars' magnetospheres. However, the natural timescales for such changes are milliseconds (Alfvén or elastic wave crossing times) and millions of years (magnetic field motion or decay), and there is no evidence that they have any effect on the precision of timing binary orbits (timescales of hours to years).

Secular effects (as are discussed in §§2 and 3) can be measured to even more startling precision with a stable pulsar, since the phase change they induce increases monotonically with time. If the pulsar pulse phase $\phi$ is defined so that $\phi \in [0, 1]$ covers a whole pulse period, then

$$\phi = \int_0^t \frac{\mathrm{d}t'}{P(t')} = \frac{t}{P(0)} - \tfrac{1}{2}\dot{P}(0)\left(\frac{t}{P(0)}\right)^2 + \tfrac{1}{6}[2\dot{P}(0)^2 - P(0)\,\ddot{P}(0)]\left(\frac{t}{P(0)}\right)^3 + \ldots, \qquad (1.1)$$

if the pulsar is monitored for a time $t$. If the pulsar phase $\phi$ is measured $N$ times during the time $t$, with a timing residual in a single measurement $P\epsilon_\phi$ (typically $\epsilon_\phi \approx 10^{-2}$), then the various terms in equation (1.1) can be fitted to a precision of order $\mathscr{F}\epsilon_\phi/\sqrt{N}$, where $\mathscr{F} \approx 20$ is a factor which accounts for the fact that many parameters are being fitted simultaneously, including the position of the pulsar on the sky (needed to remove the Earth's motion! A more complete review of fitting and the effects of noise in pulsar timing is given in Blandford *et al.* (1984)).

Beyond the Solar System, newtonian dynamics has long been known to apply to binary stars. Felix Savary is conventionally assigned the honour of being the first to show, in 1827, that a visual binary star system showed an elliptical orbit, confirming that the inverse square law applied outside the Solar System. The highest precision in determining the properties of the orbits of ordinary stars today comes from combining radial velocities (from measuring the Doppler shifts of spectral lines, which can with care give precision of $\lesssim 100$ m s$^{-1}$) with measurements of the angular separation using optical interferometers (which currently give precisions up to $\sim 0.1$ mas $\approx 5 \times 10^{-10}$ rad). Representative of the state of the art are respectively the work of Griffin (1991) and of Pan *et al.* (1992). Good precision in the orbits of bright stars gives uncertainties of 1% in the orbital eccentricities and semi-major axes, and of a few percent in the mass function and (for binaries where both components are visible) in the individual stellar masses.

To see how the properties of the orbits are deduced, consider for simplicity a binary



PHILOSOPHICAL TRANSACTIONS OF THE ROYAL SOCIETY A MATHEMATICAL, PHYSICAL & ENGINEERING SCIENCES
PHILOSOPHICAL TRANSACTIONS OF THE ROYAL SOCIETY A MATHEMATICAL, PHYSICAL & ENGINEERING SCIENCES

Downloaded from rsta.royalsocietypublishing.org



star in a circular orbit. Let the separation between the stars be $a$, and their masses be $M_1$, $M_2$. Take $M_1 > M_2$. Then (neglecting for the moment the parallax of the Earth's own orbit about the Sun) as projected on the sky each star $j$ will trace out an ellipse with semi-major axis $a_j/D$ and semi-minor axis $a_j \cos i/D$, where $D$ is the distance from Earth to the binary, $i$ is the inclination, defined as the angle between the line of sight to Earth and the normal to the orbital plane ($i = 90°$ for an orbit seen edge-on), and $a_1 = aM_2/(M_1+M_2)$, $a_2 = aM_1/(M_1+M_2)$. If the stars carry clocks ticking with intrinsic period $P_0$ (which may be atoms or a pulsar rotation period), then to newtonian order, the Doppler shifts allow us to determine the radial velocity from the observed clock tick period:

$$P = (1 + V_l/c)\, P_0. \tag{1.2}$$

Here $V_l$ is the component of the relative velocity $(\boldsymbol{V}_j - \boldsymbol{V}_\oplus)\cdot\boldsymbol{n}$ between the clock-carrying star and Earth, measured along the unit vector $\boldsymbol{n}$ to the star from the Earth, whose velocity is $\boldsymbol{V}_\oplus$. If we refer the velocity not to the Earth frame but to the Solar System barycentre (i.e. remove the contributions of the Earth's orbital and rotational velocities), then for a star on a circular orbit, the radial velocity $V_l$ will vary sinusoidally, as

$$V_{l,j} = K_j \cos(\omega+\theta) = \frac{2\pi a_j \sin i}{P_\mathrm{b}} \cos(\omega+\theta). \tag{1.3}$$

In this, $\theta = (2\pi/P_\mathrm{b})\, t$, $P_\mathrm{b}$ is the orbital period of the binary, and $t$ is newtonian universal time.

Observations of the clock frequency as a function of time thus allow one to determine $P_\mathrm{b}$ and $a_j \sin i$ (and also the orbital eccentricity $e$ and the angle $\omega$ between the line of nodes and the line of apsides, in the more general case of an elliptical orbit, whose equations are slightly more complicated – see any classical astronomy textbook, and the nice figures in King (1920)). Then combining (1.3) with Kepler's third law: $G(M_1+M_2) = (2\pi/P_\mathrm{b})^2 a^3$, we get the two equivalent forms

$$Gf(M_1,M_2) = \frac{(GM_2 \sin i)^3}{(GM_1+GM_2)^2} = \frac{PK_1^3}{2\pi} = (a_1 \sin i)^3 \left(\frac{2\pi}{P_\mathrm{b}}\right)^2, \tag{1.4}$$

if the velocity of $M_1$ is measured (exchange subscripts 1 and 2 if that of $M_2$ is measured). The quantity $f(M_1,M_2)$ is known as the mass function, and is tabulated for the binary pulsars in tables 2 and 3. Note that we have multiplied all masses by Newton's gravitational constant $G$, since $G$ is known in (MKS) units only to four significant figures. But from Solar System measurements, $G$ is known in (metres, solar masses, seconds) to enormous precision. The masses of celestial bodies (as $GM_i/GM_\odot$) are thus defined in solar masses much more precisely than in kilograms.

For pulsars, there are two ways to determine $a_\mathrm{p} \sin i$ ($a_\mathrm{p}$ is the semi-major axis of the pulsar's orbit about the binary's centre of mass). The first, and less accurate method is simply to determine the pulse period in each observing session. Equation (1.2) then determines $V_l$ for each session, and (1.3) then determines $a_\mathrm{p} \sin i$ just as in optical spectroscopic observations. This method is often used to generate initial rough orbits, and when scintillation makes the pulsar's flux too erratic to phase connect the signal. The second, and more accurate method requires counting individual pulses as in equation (1.1). One then measures the delays in the arrival of



PHILOSOPHICAL TRANSACTIONS OF THE ROYAL SOCIETY A MATHEMATICAL, PHYSICAL & ENGINEERING SCIENCES
PHILOSOPHICAL TRANSACTIONS OF THE ROYAL SOCIETY A MATHEMATICAL, PHYSICAL & ENGINEERING SCIENCES

Downloaded from rsta.royalsocietypublishing.org



the $n$th pulse. The delay is just the light travel time across the orbit: for circular orbits,

$$\Delta t = a_{\rm p}\, c^{-1} \sin i \sin(\omega + \theta), \tag{1.5}$$

which can also be obtained by integrating equation (1.3). Thus measuring $\Delta t(t)$ allows one to determine $a_{\rm p} \sin i$ and $P_{\rm b}$ and hence the mass function (1.4).

Of particular interest to us is the measurement of small eccentricities in nearly circular orbits. As Hipparcus discovered, a slightly eccentric orbit can be described as a circular orbit, with a superposed epicyclic motion of semi-amplitude along the line of sight $\frac{1}{2}ea_1 \sin i$, with twice the orbital frequency (twice, because the epicyclic variation in radius, at the orbital frequency, is multiplied by the sine of the angle to the line of sight, which also varies at the orbital frequency, and products of trigonometric functions vary at the sum and difference (here 0) of their frequencies). Thus, as a function of orbital phase, the difference in pulse arrival times between a pulsar in a circular orbit and one with a small $e$ will be

$$\delta t = \Delta t(t) - \Delta t_{\rm circ}(t) = (ea_{\rm p}/2c) \sin i\, [\sin\omega + \sin(4\pi t/P_{\rm b} - \omega)]. \tag{1.6}$$

Thus for a typical binary pulsar with $a_{\rm p} \sin i/c = 10$ s, timing accuracy of 1 μs allows us to detect $e$ as small as 1 $\mu$s/10 s $= 10^{-7}$, some five orders of magnitude more precise than the $\Delta e \approx 10^{-2}$ obtained in most optical measurements of spectroscopic binaries. This precision has interesting consequences which we explore in §7.

Observations of a binary in which only one star's radial velocity can be measured (a so-called single line spectroscopic binary, such as a pulsar with an invisible companion) allow us to solve for six of the eight newtonian parameters of a binary (position and velocity relative to the centre of mass, plus two masses). To determine the remaining two parameters $(M_1/M_2, i)$, we need additional information. A double line binary (two pulsars in a binary (not yet discovered), or a pulsar plus a star with suitably narrow and measurable spectral lines (not yet any of the pulsars with optically detected companions)) would allow us to determine the ratio $M_1/M_2$, but not $i$. To solve for $i$, we need either a measurement of the pulsar's transverse velocity (provided roughly in one case by Lyne (1984) by using scintillation pattern speeds) or a map of the orbit projected on the sky (i.e. a visual binary, not yet done, but perhaps feasible someday with optical interferometers. One would solve for $i$ by comparing the actual eccentricity from the radial velocity curve with that of the projected orbit). Alternatively, in close binaries, one can sometimes detect the non-newtonian effects of general relativity (the rate of advance of periastron gives $M_1 + M_2$; gravitational time delays give $i$ and the individual masses, as discussed by Taylor and by Damour in this symposium).

In §2 I show how the $\dot{P}$ of a pulsar is affected by its acceleration, and I show that this allows us to determine cluster mass-to-light ratios in a distance- and model-independent fashion. I use this and the radial distribution of pulsars in the globular star cluster M15 to constrain the central density and stellar composition of the core of M15. In §3 I show that in a globular cluster, the changing accelerations caused by passing stars can produce observable $\ddot{P}$s, which directly constrain the mass density in a pulsar's local environment. In §4 I discuss the consequences of stellar evolution for the orbits of pulsars recycled by mass transfer from their companions, and compare the predicted core mass-period relation with the observed properties of binaries in the Galactic disc and globular clusters. In §5 I discuss the effects of passing stars on binary pulsars. I derive cross sections for the eccentricities so induced, and discuss ionization, exchange, and the hardening and recoil of binaries



PHILOSOPHICAL TRANSACTIONS OF THE ROYAL SOCIETY A MATHEMATICAL, PHYSICAL & ENGINEERING SCIENCES
PHILOSOPHICAL TRANSACTIONS OF THE ROYAL SOCIETY A MATHEMATICAL, PHYSICAL & ENGINEERING SCIENCES

Downloaded from rsta.royalsocietypublishing.org



after encounters. In §6 I discuss the problem of recycling pulsars in low density globular clusters. I show how exchanges and resonant three- and four-body encounters involving primordial binaries may solve the problem, and explain the unusually large numbers of pulsars in globular clusters like 47 Tuc and Ter 5.

In §7 I prove that the fluctuating density of a convective star produces time-dependent moments of quadrupole and higher order. If the star is in a binary, these fluctuating moments pump the eccentricity of the orbital motion, while dissipation of the time-dependent tide tends to damp the eccentricity of the orbit. I prove that if the convection is confined to a single thin layer, a (statistical) equilibrium eccentricity is reached when the energy of the orbital epicyclic motion is equal to the energy in a single convective eddy. I show that the predictions of this theory are in good agreement with the measured eccentricities of the orbits of pulsars with white-dwarf companions. Without the pumping by the fluctuating potential, I show that tidal damping alone would have produced orbits with much smaller eccentricities than are observed. Perturbations by passing stars and mass loss at the end of the red-giant progenitor's life are inadequate to induce the observed eccentricities. In §8 I discuss the dynamics of the planets around PSR1257+12. Section 9 presents a brief conclusion. Three tables give parameters of all binary and globular cluster pulsars publicly announced at the time of writing.

## 2. Acceleration, $\dot{P}$ and surface density

An accelerated pulsar has a time-varying Doppler shift, and thus a changing period. If we transform the period measured at a telescope to the period $P$ which would be measured at the Solar System barycentre (velocity $\boldsymbol{V}_\mathrm{b}$), then the period is given by (1.2) with $V_l = (\boldsymbol{V}_\mathrm{p} - \boldsymbol{V}_\mathrm{b})\cdot\boldsymbol{n}$, where $\boldsymbol{V}_\mathrm{p}$ is the pulsar velocity and $\boldsymbol{n}$ is the unit vector pointing from the barycentre to the pulsar. Differentiating, we obtain

$$\frac{\dot{P}}{P} = \frac{\dot{P}_0}{P_0} + \frac{(\boldsymbol{a}_\mathrm{p} - \boldsymbol{a}_\mathrm{b})\cdot\boldsymbol{n}}{c} + \frac{V_\perp^2}{cD}, \tag{2.1}$$

where $\boldsymbol{a} = \dot{\boldsymbol{V}}$ is the acceleration, $D$ is the distance between the pulsar and the solar system barycentre, and $V_\perp$ is the component of the relative velocity perpendicular to $\boldsymbol{n}$, i.e. $\mu D$, where $\mu$ is the pulsar proper motion.

The third (proper motion) term in (2.1) is strictly positive, and the first term should be too (pulsars slow down as they lose rotational energy). Thus a negative $\dot{P}$ can be produced only if the acceleration (second) term is negative and dominates the other terms.

The first term in (2.1) is just the reciprocal of twice the pulsar's (intrinsic) characteristic age $\tau_0$. The third term is

$$2.4\times10^{-18}\ \mathrm{s^{-1}}\left(\frac{V_\perp}{150\ \mathrm{km\ s^{-1}}}\right)^2 \Big/ D_\mathrm{kpc} \approx \left(\frac{1}{10^{10}\ \mathrm{years}}\right)\left(\frac{V_\perp}{150\ \mathrm{km\ s^{-1}}}\right)^2 \Big/ D_\mathrm{kpc}. \tag{2.2}$$

The Galactic contributions to the second term are similar in size. If we approximate the Galaxy's potential as that of a spherically symmetric isothermal sphere, with a flat rotation curve of velocity $V_\mathrm{c} \approx 220$ km s$^{-1}$, then a pulsar at Galactic longitude $l$, latitude $b$ and distance $D \equiv R_0\,\delta$ has

$$\left.\frac{(\boldsymbol{a}_\mathrm{p} - \boldsymbol{a}_\mathrm{b})\cdot\boldsymbol{n}}{c}\right|_\mathrm{Gal} = -A_\odot\left[\cos b\cos l + \frac{\delta - \cos b\cos l}{1+\delta^2 - 2\delta\cos b\cos l}\right], \tag{2.3}$$

Downloaded from rsta.royalsocietypublishing.org



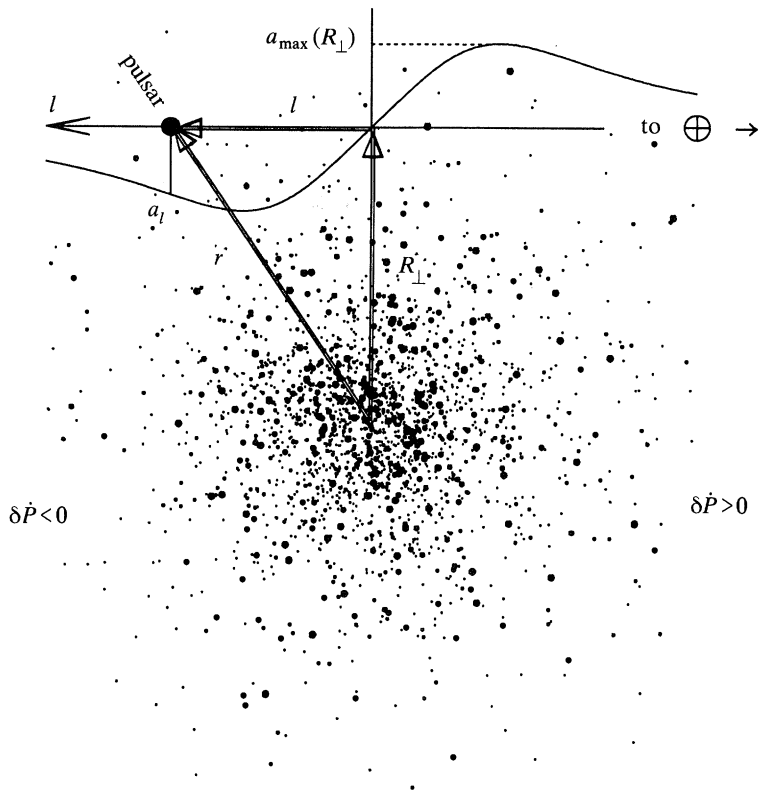


Figure 1. Schematic illustration of the line of sight component $a_l$ of a pulsar's acceleration by a star cluster, as a function of the distance $l$ between the pulsar and the sky-plane through the cluster centre. $l$ is defined positive when the pulsar is behind the centre. For any given projected distance $R_\perp$ of the pulsar, there is a maximum possible $a_l$.

where $R_0 \approx 7.5$ kpc is the Sun's Galactocentric distance, and $A_\odot = V_c^2/(cR_0) = 7\times10^{-19}\ \mathrm{s}^{-1} = 2.2\times10^{-11}\ \mathrm{a}^{-1}$. Thus the Galactic and proper-motion contributions cannot dominate the intrinsic $\dot{P}_0$ except for pulsars with characteristic ages older than the universe (or perhaps a bit less if they are unusually close to Earth or the Galactic centre).

If the pulsar lies near the centre of a dense star cluster, however, the pulsar acceleration can be substantially larger. Neglecting the Galactic and proper-motion contributions (2.2), (2.3), we have for a spherical star cluster

$$\frac{\dot{P}}{P} = \frac{\dot{P}_0}{P_0} - \frac{1}{c}\frac{GM(<r)}{r^2}\frac{l}{r}, \tag{2.4}$$

where $r = \sqrt{(R_\perp^2 + l^2)}$, and $l$ is the distance between the pulsar and the plane of the sky which passes through the centre of the cluster (see figure 1). If the pulsar has $\dot{P} < 0$, then the second term must dominate, and $l > 0$ (the pulsar lies in the back half of the cluster). One can observe $R_\perp$, but not $l$. However, the absolute value of the second term in (2.4) vanishes if $l = 0$ (acceleration perpendicular to the line of sight) or $|l| = \infty$ (no acceleration), and reaches a maximum (see figure 1) at an intermediate value of $|l|$, typically of order $\sqrt{(R_\perp^2 + r_c^2)}$, where $r_c$ is the cluster core radius. The maximum over $l$, for given $R_\perp$ of the second term $a_l/c \equiv G(M<r)\,l/r^3$ depends only

Downloaded from rsta.royalsocietypublishing.org



on the cluster's mass profile, but the probability of each $l$ and hence of each $a_l$ depends on the radial density profile of the pulsar distribution. The $\max(|a_l|)$, and probability distributions $p(|a_l|\,|\,R_\perp)$ have been computed by Phinney (1992) for many model clusters, ranging from simple powerlaw and King models to numerical multi-mass Fokker–Planck models. Two useful rules of thumb emerged from these calculations. First, to within about 10% accuracy, at all projected radii in all model clusters,

$$\max|a_l| \approx 1.1G\bar{\Sigma}(<R_\perp) = 1.1GM_{\rm cyl}(<R_\perp)/\pi R_\perp^2, \tag{2.5}$$

where $M_{\rm cyl}$ is the mass within a cylindrical tube of radius $R_\perp$ along the line of sight through the cluster centre. Observations of the surface brightness of the globular cluster tell us directly the total luminosity within similar cylindrical tubes. If a pulsar has $\dot{P}/P < 0$, then (2.1) and the discussion following it tells us that

$$\left|\frac{\dot{P}}{P}\right| < \frac{|a_l|}{c} < \frac{a_{\max}}{c} = \frac{1.1G\bar{\Sigma}(<R_\perp)}{c} = 5\times10^{-16}\left(\frac{\bar{\Sigma}}{10^6\,M_\odot\ \mathrm{pc}^{-2}}\right)\mathrm{s}^{-1}. \tag{2.6}$$

Hence the ratio of the observed negative $\dot{P}/P$ to the observed surface density gives us directly a strict lower limit to the mass-to-light ratio of the cluster within the cylinder on which the pulsar is projected. In fact, even the distance to the globular cluster cancels out in the ratio. A less precise rule of thumb (good only to $\sim 50\%$) is

$$\frac{\max|a_l(R_\perp)|}{c} \approx \frac{1}{c}\frac{\sigma(R_\perp)^2}{\sqrt{(r_c^2+R_\perp^2)}} \approx 10^{-17}\left(\frac{\sigma(R_\perp)}{10\ \mathrm{km\ s}^{-1}}\right)^2\frac{1\ \mathrm{pc}}{\sqrt{(r_c^2+R_\perp^2)}}\,\mathrm{s}^{-1}, \tag{2.7}$$

where $\sigma(R_\perp)$ is the line-of-sight velocity dispersion of giant stars at the pulsar position, and $r_c$ is the cluster core radius.

Another useful rule of thumb is that for most realistic radial pulsar distributions and clusters, the distribution of acceleration below the maximum (2.5) is

$$p(|a_l| > a\,|\,R_\perp) = 1-(2/\pi)\arcsin(a/a_{\max}). \tag{2.8}$$

This gives a median acceleration of $0.71a_{\max}$, indicating the typical magnitude of the second inequality in (2.6).

We can apply these ideas to the globular cluster M15 (Phinney 1992). This cluster has one of the highest known central luminosity densities. The two pulsars closest to its core, PSRs 2127+11A,D (figure 2), both have $\dot{P}/P = -2\times10^{-16}\ \mathrm{s}^{-1}$. Equation (2.6) then immediately tells us that within their projected radii $\bar{\Sigma} > 4\times10^5 M_\odot\ \mathrm{pc}^{-2}$. Recent observations with Hubble Space Telescope (Lauer *et al.* 1991) show that in $U$-band, the surface brightness of M15 is nearly constant within the central arcsecond, and the brightness profile has a core radius of 2.2 arcsec. Individual giant stars are too sparse to define a reliable central surface brightness in giants, but the central surface brightness in unresolved stars is (after correcting for dust extinction $A_U = 4.7E_{B-V} = 0.5$ (Fahlman *et al.* 1985)) $\Sigma_{c,U,ur} = 1.4\times10^5\,L_{\odot,U}\ \mathrm{pc}^{-2}$. Attaching to this a cluster-average population of giants would then give a central surface brightness $\Sigma_{c,U} = 2.3\times10^5\,L_{\odot,U}\ \mathrm{pc}^{-2}$. It is not an easy task to determine the positions of the pulsars relative to the centre of the cluster as determined from the Space Telescope image. This has been done by locating the optical counterpart of the X-ray binary, AC 211 (Naylor *et al.* 1988) on the image. A VLA radio source has been identified as its radio counterpart (Kulkarni *et al.* 1990), and an accurate transformation exists in this part of the sky between VLA coordinates and pulsar timing coordinates, allowing in this indirect way the pulsars to be localized on the optical image. Figure 2 shows the result: pulsars A and D are respectively 0.9 and 1.2 arcsec, about half a core

Downloaded from rsta.royalsocietypublishing.org



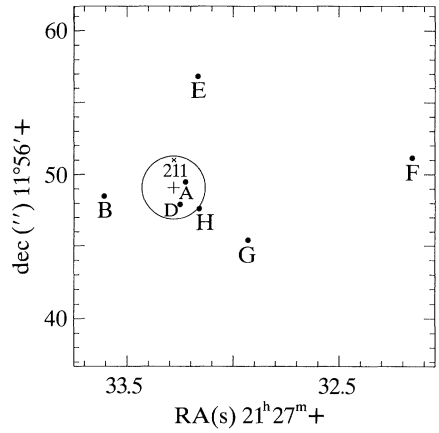


Figure 2. Positions (B1950) of the single pulsars PSR2127+11A–H in M15. PSR2127+11C is a binary, and lies outside of the plotted area (see §5). The cross and circle respectively represent the centre and core radius of unresolved stars in $U$-band light, measured by Lauer *et al.* (1991) (see text). The × marks the position of the low mass X-ray binary AC211.

radius, from the optical centre of the cluster. The distance to M15 is $10.0 \pm 1$ kpc (Fahlman *et al.* 1985; note that Lauer *et al.* (1991) quote 12.8 kpc from the same reference, but they neglected to correct the apparent distance modulus given there for extinction). Thus the core radius of 2.2 arcsec corresponds to 0.11 pc.

If the mass density profile flattens with the same core radius as the light distribution, then since PSRs 2127+11A and D are both projected well within the core, we can use the lower limit to the mass surface density from the $\dot{P}$s to compute a lower limit to the projected mass-to-light ratio in the core of M15:

$$M/L_U = \Sigma_c/\Sigma_{c,U} > 1.8 M_\odot/L_{\odot,U}, \tag{2.9}$$

with a most probable value of $1.8/0.71 = 2.5$. Since the $U$–$V$ colour of M15 is similar to the Sun's, this ratio should also apply in $V$-band. Again assuming that the mass distribution has the same core radius at the light, we also have a lower limit to the central mass density:

$$\rho_c = \Sigma_c/(2r_c) > 2 \times 10^6 M_\odot \text{ pc}^{-3}, \tag{2.10}$$

with a most probable value of $\rho_c \approx 3 \times 10^6 M_\odot$ pc$^{-3}$. If the core radius of the mass density were much less than that of the $U$-band luminosity, the mass density at the pulsars' projected radii could be about twice this high.

The rougher rule of thumb (2.7) gives a lower limit to the velocity dispersion at the position of the pulsars $\sigma(1'') \approx \sigma_c > 15$ km s$^{-1}$. More careful modelling using Fokker–Planck models with 10 mass groups (Phinney 1992; Murphy & Phinney 1992) shows that the acceleration constraints and the light profile can only be simultaneously fitted by models (e.g. figure 3) whose line of sight velocity dispersion of turn-off mass stars at 0.1 pc is in the range 13–16 km s$^{-1}$. Direct optical measurements are difficult because only a few giant stars contribute most of the light in the central few arcseconds. Thus the apparent dispersion can change dramatically if even a single star is included or excluded. Peterson *et al.* (1989) derived a dispersion $\sigma_c$ within 1″ of 25 km s$^{-1}$. No reasonable model can reconcile this with the pulsar $\dot{P}$s. However, Meylan *et al.* (1991) point out that the velocity distribution of Peterson *et al.* was not symmetric about the cluster mean, and appears to have been contaminated by one high velocity giant. Their own careful measurements over the inner 3″ give $\sigma_c = 13.7$ km s$^{-1}$, in good agreement with the models which fit the $\dot{P}$s.

Downloaded from rsta.royalsocietypublishing.org



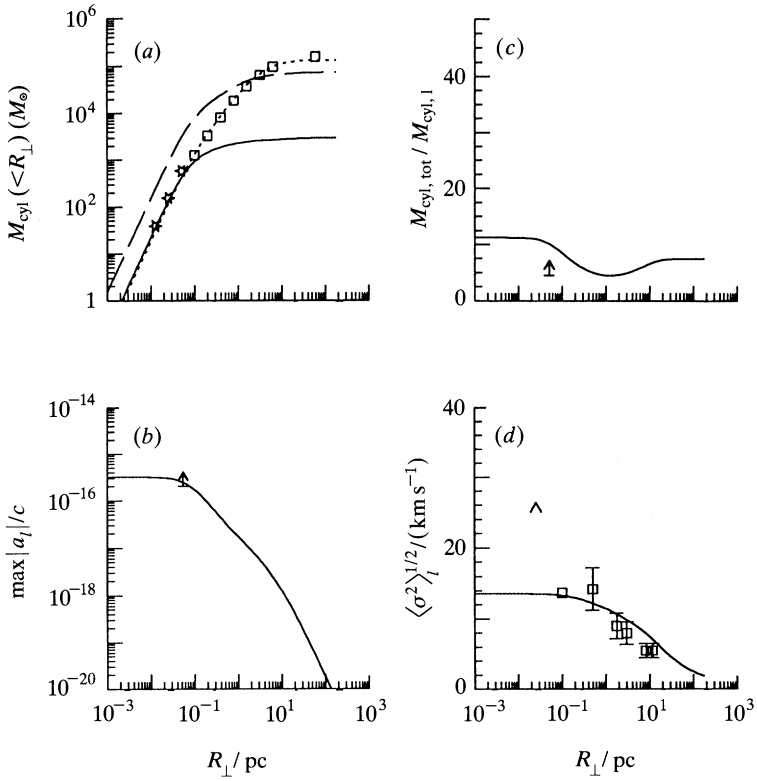


Figure 3. Data points are for the globular cluster M15. Curves show properties of a Fokker–Planck model of a globular cluster with stars in 10 mass groups representing remnants of stars with an initial mass function $dN/dm \propto m^{-(1+1.2)}$, slightly flatter than a Salpeter slope. Only 10% (1000) of the neutron stars created were retained in the cluster. The total mass today (21.4 Ga in the simulation) is $10^6 M_\odot$, and the cluster began its gravothermal collapse as a Plummer model with scale radius $r_0 = 4.5$ pc. The curves show the cluster at maximum bounce after core collapse. The code used is essentially that described in Murphy *et al.* (1990). In (*a*) masses within projected radii are shown for neutron stars and white dwarfs heavier than $1.25M_\odot$ (solid), $0.8 < M < 1.25M_\odot$ heavy white dwarfs (dashed), and $0.63 < M < 0.8M_\odot$ upper main sequence, giant and white dwarf stars (dotted). The squares are photometry of M15 (stars are Space Telescope data from Lauer *et al.* (1991)), scaled by using a mass-to-light ratio appropriate for the $0.63 < M < 0.8M_\odot$ group and the metallicity of M15. (*b*) The maximum possible line-of-sight acceleration as a function of projected radius. The arrow shows the constraint imposed by the negative $\dot{P}$s of PSRs 2127+11A,D in M15. (*c*) The ratio of total mass within a projected radius to the mass in the $0.63 < M < 0.8M_\odot$ group. The arrow shows the lower limit imposed by PSRs 2127+11A,D and the rule of thumb (2.5). (*d*) The line-of-sight integrated velocity dispersion of the $0.63 < M < 0.8M_\odot$ group. Squares with error bars are measured velocity dispersion in M15 from Peterson *et al.* (1989). Caret is central dispersion claimed by the same authors (see text). Inner square is central dispersion measured by Meylan *et al.* (1991).

### (*a*) *Relaxation and equilibrium*

The radial distribution of pulsars in M15 also provides a test of stellar dynamics. The single pulsars ($m_p \approx 1.4M_\odot$) are about twice as heavy as the $m_t \approx 0.7M_\odot$ post-turn-off and upper main sequence stars which dominate the light. Although the pulsars might preferentially be spun-up in the cluster core (e.g. by tidal capture, see §6), their characteristic ages (table 1) greatly exceed the timescale for relaxation through gravitational two-body encounters in the cluster core ($\sim 10^7$ years).

Downloaded from rsta.royalsocietypublishing.org



Table 1. *Pulsars in globular clusters*

(Clusters are in order of decreasing central density. Those above the line are post core collapse (PCC) or nearly so, and also contain a bursting X-ray source (an accreting neutron star). The reference number is followed by the first letter of the author's last name to facilitate location in the reference list.)

| cluster | $\rho_c$[b] / $L_{\odot V}$ pc$^{-3}$ | $\sigma_c$[c] / km s$^{-1}$ | pulsar | $P$ / ms | bin ? in table 2 | $\dot{P}$ / ss$^{-1}$ | $P/(2\dot{P})$ / years | ref. |
|---|---|---|---|---|---|---|---|---|
| M15 | $1\times10^6$ | 15 | 2127+11A | 110.7 | single | $-10^{-16.7}$ | $>10^{8a}$ | 1A |
| | | | 2127+11B | 56.1 | single | $10^{-17.1}$ | $10^{8.3}$ | 1A |
| | | | 2127+11C | 30.5 | binary | $10^{-17.3}$ | $10^{8.3}$ | 2P |
| | | | 2127+11D | 4.6 | single | $-10^{-18.0}$ | $>10^{8a}$ | 2P |
| | | | 2127+11E | 4.8 | single | $10^{-18.7}$ | $10^{8.6}$ | 2P |
| | | | 2127+11F | 4.0 | single | $10^{-19.5}$ | $>10^{8.9a}$ | 3A |
| | | | 2127+11G | 37.7 | single | $10^{-17.7}$ | $>10^{8.5a}$ | 3A |
| | | | 2127+11H | 6.7 | single | $10^{-19.6}$ | $>10^{8.0a}$ | 3A |
| N6624 | $>3\times10^5$ | (12) | 1820−30A | 5.4 | single | | | 4B |
| | | | 1820−30B | 378.6 | single | | | 4B |
| N6440 | $3\times10^5$ | (14) | 1746−20 | 288.6 | single | | | 5M |
| Ter5 | $2\times10^5$ | (12) | 1744−24A | 11.6 | binary | $-10^{-19.7}$ | $>10^{9.3a}$ | 6T |
| M28 | $1\times10^5$ | 9 | 1821−24 | 3.0 | single | $10^{-17.8}$ | $10^{7.5}$ | 7F |
| 47Tuc[d] | $4\times10^4$ | 12 | 0021−72C | 5.8 | single | | | 8M |
| | | | D–J,L,M | 2–5 | E,J bin | | | 9M |
| M5 | $2\times10^4$ | 5.5 | 1516+02A | 5.5 | single | $<10^{-19}$ | $>10^9$ | 10W |
| | | | 1516+02B | 7.9 | binary | | | 10W |
| N6539 | $8\times10^3$ | (5) | 1802−07A | 23.1 | binary | | | 11D |
| M4 | $8\times10^3$ | 4 | 1620−26 | 11.1 | binary | $10^{-18.1}$ | $10^{8.3}$ | 12M |
| N6760 | $6\times10^3$ | (6) | 1908+00A | 3.6 | binary | | | 13A |
| M13 | $3\times10^3$ | 8 | 1639+36A | 10.4 | single | $<10^{-19.4}$ | $>10^{9.6a}$ | 14K |
| | | | 1639+36B | 3.5 | binary | | | 15K |
| M53 | $1\times10^3$ | (6) | 1310+18 | 33.2 | binary | | | 14K |

[a] $\dot{P}$ believed (§2) to be caused by the acceleration of the pulsar in its orbit about the dense cluster core.

[b] Central visual luminosity density (from Djorgovski, personal communication). The mass-to-light ratio in the cores of low density clusters is typically $\sim 1$–$3 M_\odot/L_{\odot V}$, but can be $>10$ in the denser clusters (see §§2, 3).

[c] Central line-of-sight velocity dispersion of giant stars ($\sim 0.8 M_\odot$). When enclosed in ( ), is not measured, but estimated from fitting a King model with a typical $M/L$. References are given in Phinney (1992).

[d] The nine pulsars 0021-72D–M are only visible during moments of favourable scintillation, and have thus proved difficult to characterize and confirm. K may be simply the third harmonic of D, not a separate pulsar.

Thus gravitational encounters should have ample time to equilibrate the mean kinetic energies $kT$ of these two types of stars (see figs 3 and 4 of Murphy *et al.* (1990)). In statistical equilibrium, the number density $n_i$ of a species of mass $m_i$ in a gravitational potential $\phi(r)$ is given by the Boltzmann factor $n_i \propto \exp(-m_i\phi(r)/kT)$. Thus at given $r$, the pulsar density $n_p \propto n_t(r)^{m_p/m_i}$ should scale roughly as the square of the density of turn-off stars.

In M15, fitting the light profile outside the core gives $n_t \propto r^{-\nu(r)}$, where

$$\nu \approx 1.56 + 0.043(\ln\theta)^2, \quad \theta > 2'' \text{ in arcsec.} \tag{2.11}$$

Thus in the inner regions, we expect $n_p \propto r^{-3.1}$, i.e. nearly constant numbers in every

Downloaded from rsta.royalsocietypublishing.org



Figure 4

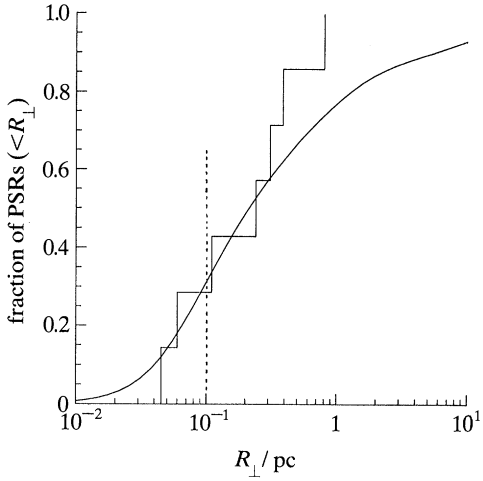


Figure 5

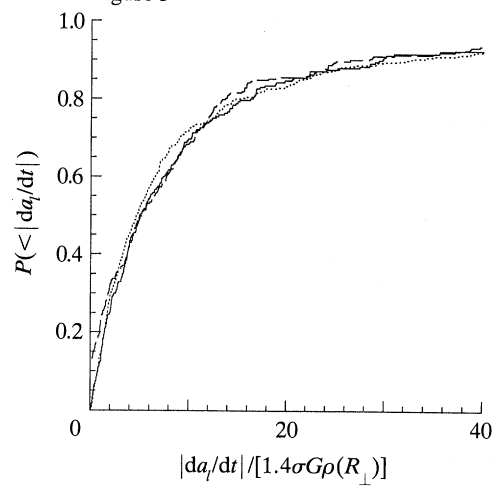


Figure 4. Histogram is the cumulative radial distribution of single pulsars in M15. The vertical dashed line is at the core radius of $U$-band light. Most pulsars lie outside the core, as expected (see text). The smooth solid line is the distribution of neutron stars in the Fokker–Planck cluster model illustrated in figure 3.

Figure 5. Cumulative distribution of gravitational jerks of $10^3$ stars drawn from a centrally concentrated distribution (see text) in a cluster whose core contains about 6000 perturbing stars (specifically simulated is a King model cluster with $W_0 = 6$ and $10^5$ stars in total $\rho_{NS} \propto \rho_*^2$, $\sigma_{NS} = \sigma/\sqrt{2}$). ——, $R_\perp < 0.5$; - - - - -, $0.5 < R_\perp < 1.5$; — —, $R_\perp > 1.5$.

logarithmic interval of radius. It is thus not surprising that five of the seven single pulsars in M15 are outside the core (see figures 2 and 4; we omit the binary PSR 2127+11C, both because it is twice as heavy, and because its formation involved ejection onto an orbit from which it has not yet been relaxed; see §5). In figure 4, we compare the radial distribution of pulsars with that of the $1.4M_\odot$ mass group in the same Fokker–Planck simulation which fits M15 in figure 3. They are comfortingly similar. Note that it would not be surprising if one of the next few single pulsars discovered in M15 lay beyond 10 core radii ($22'' = 1$ pc). Clusters with large core radii generally have steeper surface brightness profiles outside their cores than do highly concentrated ('post core collapse') clusters like M15. Most of their pulsars in equilibrium should then lie within their cores. In low density clusters, however, the relaxation time can exceed the pulsar ages, so in those the radial distribution may be determined more by the formation process than by statistical equilibrium.

Deep in a cluster's potential well, the fact that all mass species follow a Boltzmann distribution means that if one species of mass $m_d$ dominates the density over a wide range of radius, the density profile of that species must approximate an isothermal sphere, $\rho_d \propto r^{-2}$. Thus stars $i$ of higher mass than $m_d$ must have steeper density profiles, and lighter stars have a shallower density profile. In M15, (2.11) shows that the $0.7M_\odot$ turn-off stars have a shallower profile within 1 pc, and figure 4 shows that the pulsars have a steeper profile. We infer that at $r < 1$ pc, the mass density in M15 is dominated by stars of intermediate mass ($\sim 1M_\odot$, which must be heavy white dwarfs). This is indeed the case in the model of figure 3*a*. And since these are dark remnants, it nicely explains the high central mass to light ratio (see figure 3*c*). To make the required numbers of heavy white dwarfs, standard stellar evolution requires that the initial mass function in M15 have been at least at flat as the Salpeter

Downloaded from rsta.royalsocietypublishing.org



one, appropriate to Galactic star formation (Massey & Thompson 1991), $\mathrm{d}N/\mathrm{d}m \propto m^{-2.35}$ between $0.7M_\odot$ and the $M > 3M_\odot$ stars progenitors of heavy white dwarfs. Extrapolating such a slope to the masses of neutron star progenitors predicts that at least $10^4$ neutron stars were formed in M15 (though of course many could have escaped at birth).

## 3. Jerk, $\ddot{P}$ and local density

Differentiating (1.2) twice, and using $\tau_0 \equiv P_0/(2\dot{P}_0)$ and $n_0 \equiv 2-\ddot{P}_0 P_0/\dot{P}_0^2$ (the intrinsic braking index $n_0 = 3$ for a vacuum magnetic dipole model; young pulsars have measured $2 < n_0 < 3$), we have

$$\frac{\ddot{P}}{P} = \frac{(2-n_0)}{4\tau_0^2} + \frac{\dot{\boldsymbol{a}}\cdot\boldsymbol{n}}{c} + \frac{2}{\tau_0}\left[\frac{\boldsymbol{a}\cdot\boldsymbol{n}}{c} + \frac{V_\perp^2}{cD}\right] + \frac{\boldsymbol{a}\cdot\boldsymbol{V}_\perp}{Dc} + \frac{\mathrm{d}}{\mathrm{d}t}\left(\frac{V_\perp^2}{cD}\right), \tag{3.1}$$

where $\boldsymbol{a} = \boldsymbol{a}_\mathrm{p} - \boldsymbol{a}_\mathrm{b}$. The second term dominates the remaining terms in star clusters, whose crossing times are much less than the characteristic ages of their recycled pulsars and their orbital periods in the galaxy. It also generally dominates the first term. Thus all pulsars in globular clusters should have $\ddot{P}/P = (1/c)\,\mathrm{d}a_l/\mathrm{d}t$. This effect was first pointed out by Blandford *et al.* (1987), after the discovery of the first globular cluster source, but before it was shown to be a pulsar.

If we consider a pulsar in the core of a star cluster, where $\rho(r) \approx \rho_0$, then the mean field acceleration is $\boldsymbol{a}_\mathrm{mf} = \frac{4}{3}\pi G\rho_0 \boldsymbol{r}$. Differentiating and taking the line-of-sight component then gives the mean field contribution

$$(\ddot{P}/P)_\mathrm{mf} = \tfrac{4}{3}\pi G\rho_0\, v_l/c = 6\times10^{-28}\,\rho_6\, v_{10}\ \mathrm{s}^{-2}, \tag{3.2}$$

where $\rho_0 = 10^6\,\rho_6\,M_\odot\ \mathrm{pc}^{-3}$ and $v_l = 10 v_{10}\ \mathrm{km\ s}^{-1}$. From equation (1.1), $\ddot{P}/P$ can be measured to $6\times10^{-28}$ in about a year of timing with 1 μs residuals. So this effect should be measurable, at least in the denser globular clusters.

The interpretation of a pulsar's jerk, however, is complicated by the fact that its nearest neighbours make a contribution comparable with that of the mean field. The exact expression for the $\alpha$ component ($\alpha$ runs over $x$, $y$, $z$) of the pulsar's jerk is

$$\dot{a}_{\mathrm{p},\alpha} = \sum_i GM_i \frac{(v_i - v_\mathrm{p})_\beta}{|r_i - r_\mathrm{p}|^3}\left[\delta_{\alpha\beta} - \frac{3(r_i-r_\mathrm{p})_\alpha (r_i-r_\mathrm{p})_\beta}{|r_i-r_\mathrm{p}|^2}\right]. \tag{3.3}$$

The pulsar's nearest neighbour has a median $|r_i - r_\mathrm{p}| \sim (\rho/M_i)^{-\frac{1}{3}}$, so its contribution to (3.3) is $\dot{a}_{l,nn} \sim G\rho(v_i - v_\mathrm{p})_l$, of the same order as the mean field contribution (3.2). To compute the distribution of jerks a given pulsar would feel thus requires Monte Carlo simulation. We have carried out such simulations, directly summing equation (3.3) for pulsars placed in self-consistent King model clusters. In the simulations, following the discussion of §2, we have drawn the pulsars from a density distribution which varies as the square of that of the perturbing stars, and a velocity distribution with variance half that of the perturbing stars. In figure 5 we show the resulting cumulative distribution of jerks. This distribution is invariant to scalings of the total number of stars in the cluster and the cluster concentration, which keep the number of stars in the core constant. The simulation shown is roughly correct to M15. To estimate the expected $\ddot{P}/P$ for PSRs 2127+11A,D, we take $\rho(0.5r_\mathrm{c}) \approx 3\times10^6\,M_\odot\ \mathrm{pc}^{-3}$ from equation (2.10). Then figure 5 gives a median expected $\ddot{P}/P = 4\times10^{-27}\ \mathrm{s}^{-2}$, and 80% of the time $\ddot{P}/P < 1.4\times10^{-26}$. Note that the timescale for $\ddot{P}$ to change is that for the nearest neighbour to change its position, of order

Downloaded from rsta.royalsocietypublishing.org



$\sigma^{-1}(\rho_c/M_i)^{-\frac{1}{3}} \sim 10^3\,\rho_6^{-\frac{1}{2}}\,v_{10}^{-1}$ years, or about a century for pulsars in the core of M15. The nearest star passing by a pulsar typically dominates the third and higher derivatives of $P(t)$. Measurement of these higher derivatives thus would allow one to solve for the mass function and parameters of its hyperbolic orbit.

## 4. Stellar evolution

Stars begin their lives by fusing hydrogen to helium in their central regions. As time goes on, a core region develops in which all the available hydrogen has been exhausted. As the central heat source wanes, the outer layers of the star are compressed by gravity until fusion begins in the regions outside the core (which initially were at too low a temperature and density to have significant fusion). In stars of mass $M \lesssim 2M_\odot$, the growing core is supported by electron degeneracy pressure, and hence becomes smaller as the core mass $M_c$ increases. The gravity at the core's surface becomes enormous, so hydrostatic equilibrium implies that the pressure gradient in the hydrogen burning layer at its surface is extremely steep. Consequently the envelope above the layer has very little effect on the layer's temperature, density, and rate of hydrogen fusion (and hence on the luminosity of the star). As the core becomes smaller and more massive, hydrostatic equilibrium in the hydrogen-burning shell requires its temperature to increase. Because of the steep temperature dependence of nuclear reaction rates, this means that the luminosity of the burning shell increases rapidly with core mass (a nice discussion may be found in Refsdal & Weigert (1970)). For the reason mentioned above, this relation $L(M_c)$ is almost independent of the properties of the overlying envelope.

The large temperature gradient above the shall also makes the envelope above the hydrogen burning shell fully convective up to the photosphere of the star. Since the specific entropy is kept almost constant by convection, equating $p(T)$ for the isentropic envelope to the photospheric pressure $p \sim G(M_c + M_{env})/(R^2\kappa(p, T_{eff}))$ gives a unique solution for $T_{eff}(R, M_c, M_{env})$, the so-called Hayashi track. Since the stellar luminosity $L \propto R^2\,T_{eff}^2$, this is equivalent to a unique solution for $R(L, M_c, M_{env})$. Here $\kappa$ is opacity, and $M_{env}$ is the mass in the envelope above the hydrogen burning shell. This relation applies while $M_{env} > 0.04(M_c/0.2\,M_\odot)^{-3.5}\,M_\odot$. When the envelope mass drops below this limit (a few times the mass of the burning shell), the envelope begins to shrink. Combined with the $L(M_c)$ relation, this gives a unique relation for $R(M_c \approx M)$ at the moment that the envelope of the giant collapses at the end of mass transfer. If the giant at this moment is just filling its Roche lobe (radius $R_L$) in a binary, as it must be for stable mass transfer, its radius $R = R_L$ and mass $M \approx M_c$ determine the orbital semi-major axis and hence, from Kepler's third law, the orbital period $P_b$. This $P_b(M_c)$ relation, whose importance was emphasized by Refsdal & Weigert (1971) and by Joss *et al.* (1987), is plotted in figure 6. The smooth solid curve is the fitting function of eq. (10) of Joss *et al.* (1987). The slightly irregular solid and dotted curves near it are stellar models from Sweigert & Gross (1978). Plotted also are the companion masses and orbital periods of the binary pulsars listed in tables 2 and 3 which have small orbital eccentricities.

The giant companions to globular cluster sources have much lower abundances by weight $Z$ of elements heavier than helium ('metallicities') than do those of Galactic pulsars. Hence their $P_b(M_c)$ should be compared with the dashed curves in figure 6, not to the solid ones. The fact that at a given core mass, low metallicity giants are smaller (hence smaller $P_b$ when Roche-lobe filling) is due in large part to the fact that



PHILOSOPHICAL TRANSACTIONS OF THE ROYAL SOCIETY A MATHEMATICAL, PHYSICAL & ENGINEERING SCIENCES
PHILOSOPHICAL TRANSACTIONS OF THE ROYAL SOCIETY A MATHEMATICAL, PHYSICAL & ENGINEERING SCIENCES

Downloaded from rsta.royalsocietypublishing.org



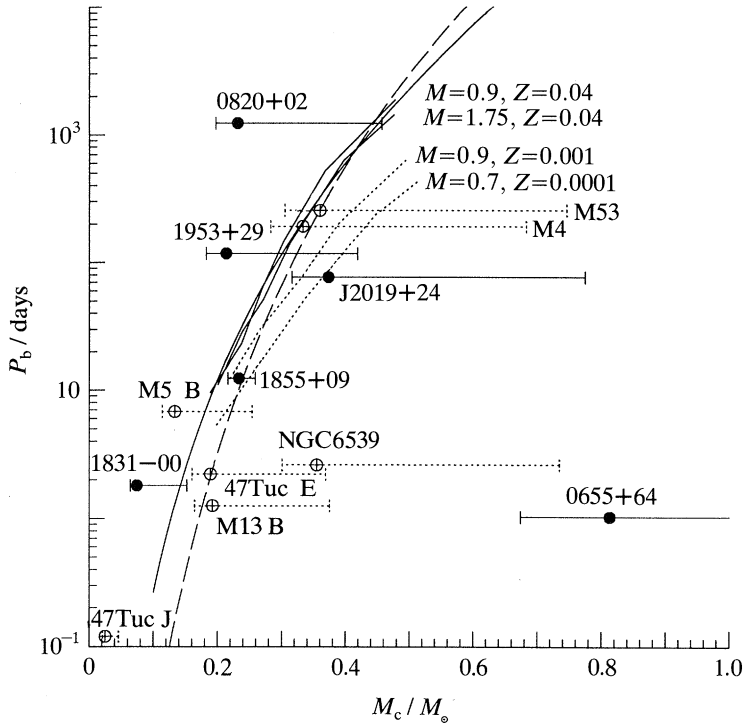


Figure 6. Predicted relation between core mass (i.e. final white dwarf mass) and orbital period for binaries containing a $1.4M_\odot$ neutron star, in which a giant star of the given core mass fills its Roche lobe. The curves (described in text) were computed for stars of different metallicities $Z$. The dotted curves are for $Z$ appropriate for globular clusters. The filled circles show the mass (or allowed mass range) of the companions of binary pulsars in the Galactic disc which have nearly circular orbits. The open circles with dotted mass ranges represent companions of binary pulsars in globular clusters. See text for discussion of NGC6539 and PSR0655+64.

the Hayashi track depends on the photospheric opacity. Lower metallicity gives a lower opacity, and a higher photospheric pressure. This in turn means that $R$ at given $L$ is lower for lower metallicity. However, the models (Sweigert & Gross 1978) also show a small additional effect in the same direction from the fact that the low metallicity stars also have smaller luminosities at a given core mass.

Most pulsars in circular binaries have companions with masses and periods compatible with the predicted relations. This is true of pulsars both in clusters and in the galactic disc, suggesting that the circular binaries did go through a phase in which the pulsar's companion filled its Roche lobe and spilled matter onto the pulsar. However, two binary pulsars clearly do not fall on the Roche lobe $P_b$–$M_c$ relation. The first is PSR0655+64. Its companion is so massive that conservative mass transfer would have been dynamically unstable (Hjellming & Webbink 1987), and the neutron star would have rapidly spiralled into the giant's envelope. Friction would simultaneously remove orbital angular momentum and eject the envelope. Thus its high mass and short orbital period are not surprising, though the physics of spiral-in are poorly understood. The second is PSR1802−07A in the globular cluster NGC 6539, whose orbit is much too small to have contained a giant with core mass equal to the companion's mass. The orbit is also very eccentric, $e = 0.22$, suggesting either that it was never circularized (companion never filled its Roche lobe), or was

Downloaded from rsta.royalsocietypublishing.org



Table 2. *Binary radio pulsars in globular clusters*
(Clusters are in order of decreasing central density, as in table 1.)

| cluster | pulsar | $P$ / ms | $P_b$ / d | $e$ | $f(M)^a$ / $M_\odot$ | $M_2{}^c$ / $M_\odot$ | ref. |
|---|---|---|---|---|---|---|---|
| M15 | 2127+11C | 30.5 | 0.33 | 0.68 | 0.153 | 1.3 | 2P |
| Ter5 | 1744−24A | 11.6 | 0.08[d] | $< 10^{-3}$ | $3.22 \times 10^{-4}$ | (0.09) | 6T |
| 47Tuc | 0021−72E | 3.5 | 2.22 | $< 0.1$ | $1.7 \times 10^{-3}$ | (0.16) | 9M |
| 47Tuc | 0021−72J | 2.1 | 0.12[d] | $< 0.03$ | $4.9 \times 10^{-6}$ | (0.02) | 9M |
| M5 | 1516+02B | 7.9 | 6.8[b] | 0.13[b] | $6.5 \times 10^{-4}$ | (0.11) | 15K |
| N6539 | 1802−07A | 23.1 | 2.62 | 0.21 | $9.5 \times 10^{-3}$ | (0.30) | 11D |
| M4 | 1620−26 | 11.1 | 191.44 | 0.025 | $8.0 \times 10^{-3}$ | (0.28) | 12M |
| N6760 | 1908+00A | 3.6 | 0.14[b] | 0.0[b] | $2.9 \times 10^{-6}$ | (0.02) | 16D |
| M13 | 1639+36B | 3.5 | 1.26[b] | 0.0[b] | $1.81 \times 10^{-3}$ | (0.16) | 15K |
| M53 | 1310+18 | 33.2 | 255.84 | $< 0.01$ | $9.79 \times 10^{-3}$ | (0.31) | 14K |

[a] Mass function $f(M) = (M_2 \sin i)^3 \, (M_2 + M_{psr})^{-2}$.
[b] Provisional parameters: no phase-connected solution.
[c] Mass of pulsar's companion (when in parentheses, tabulated value is $M_2 \sin i$, computed from the mass function $f$ in the preceding column assuming a pulsar mass of $1.4 M_\odot$).
[d] Pulsar eclipsed when behind companion (or its wind).

shrunk and made eccentric by encounters with passing stars. As described in the next two sections, the first possibility is more likely.

## 5. Effect of passing stars on binaries

One clue to the origin of the binary pulsars in globular clusters is provided by the eccentricities of the binary orbits. Since the pulsars generally have characteristic ages much less than the $\gtrsim 10^{10}$ years ages of the globular clusters in which they lie, they must recently have acquired angular momentum by accretion. The remarkably low masses of the binary pulsars' companions (table 2) suggest that the companions supplied the accreted matter. While the neutron star is close enough to its companion to pull matter from its surface, the neutron star will also exert strong tidal forces on the companion. As described in §7, if the orbit is initially non-circular, the resulting time-dependent tide will dissipate energy in the companion, circularizing the orbit. The Galactic binary pulsars with low-mass white dwarf companions have clearly had their orbits circularized in this manner (see table 3 and §7). By contrast, many of the cluster pulsars have much larger eccentricities (see table 2) than those of the seemingly similar Galactic counterparts. Furthermore, the ratio of numbers of single to binary recycled pulsars is much larger in globular clusters (17:11) than in the Galactic disc (1:12), with the ratio being especially high in the clusters with the highest central densities. This suggests that passing stars may be influencing the orbits of cluster pulsars after the completion of the mass transfer which led to their reactivation.

### (*a*) *Eccentricities*

Consider a perturbing mass $M_p$ which passes at velocity $V_p$ within a distance $R_p$ of a binary whose components $M_1$, $M_2$ are in a circular orbit of radius $a \ll R_p$, with orbital period $2\pi/\Omega_b$. For simplicity, we consider only encounters in which all bodies orbit in a single plane. We let $\mu = M_p/(M_1+M_2)$, and define a parameter $\lambda = \Omega_b R_p / V_p$. If $\lambda \ll 1$, then the encounter lasts much less than one orbital

Downloaded from rsta.royalsocietypublishing.org



Table 3. *Binary and millisecond pulsars in the Galaxy*

(The horizontal lines divide the pulsars into five groups, depending on their probable evolutionary history. In the first group, 1259−63 has a visible Be star as companion. The remaining pulsars in that group have high mass, probably neutron star (though 1820−11 may be lower main-sequence (Phinney & Verbunt 1991)) companions in eccentric orbits, and could have originated from binaries composed of two massive stars. The second group has a high mass white dwarf companion, which must have formed in a massive red giant much larger than the current orbit, implying that the neutron star spiralled into, and ejected the giant's envelope during unstable mass transfer. The third group has low mass white dwarf companions in circular orbits, which could have formed in stable accretion from low mass companion stars filling their Roche lobes. The residual eccentricities are discussed in §5. The fourth group consists of systems with companions less massive than the core mass ($\sim 0.16 M_\odot$) of the least massive star to have evolved off the main sequence in the age of the universe. Their mass transfer must have been driven by something other than nuclear evolution of the companion: e.g. gravitational radiation, or loss of angular momentum in a magnetic wind. In the fifth group, 1937+21 is single, and 1257+12 seems to have a planetary system. These pulsars seem to have destroyed the stellar companions which provided the angular momentum to spin them up.)

| pulsar | $P$ ms | $P_b$ d | $e$[a] | $f(M)$[b] $M_\odot$ | $M^2$[c] $M_\odot$ | $\log_{10}(B/\mathrm{G})$[d] | $P/(2\dot{P})$ years | ref. |
|---|---|---|---|---|---|---|---|---|
| 1259−63 | 47.8 | $> 10^3$ | $> 0.97$ | $\sim 10$ | $\sim 20$ | | | 17J |
| 1820−11 | 279.8 | 358 | 0.794 | 0.068 | (0.8) | 11.8 | $3\times10^6$ | 18L |
| 1913+16 | 59.0 | 0.32 | 0.617 | 0.132 | 1.39 | 10.4 | $1\times10^8$ | 19T |
| 1534+12 | 37.9 | 0.42 | 0.274 | 0.315 | 1.36 | 10.0 | $2\times10^8$ | 20W |
| 2303+46 | 1066.4 | 12.3 | 0.658 | 0.246 | 1.5 | 11.9 | $3\times10^7$ | 21L |
| 0655+64 | 195.7 | 1.03 | $7\times10^{-6}$ | 0.071 | (0.8)[f] | 10.1 | $5\times10^9$ | 22J |
| 0820+02 | 864.8 | 1232 | 0.0119 | 0.0030 | (0.23)[f] | 11.5 | $1\times10^8$ | 23T |
| 1953+29 | 6.1 | 117 | 0.00033 | 0.0024 | (0.21) | 8.6 | $3\times10^9$ | 24R |
| J2019+24 | 3.9 | 76.5 | 0.000111 | 0.0107 | (0.37) | 8.7 | $1\times10^9$ | 25T |
| 1855+09 | 5.4 | 12.3 | 0.000021 | 0.0056 | 0.23[f] | 8.5 | $5\times10^9$ | 26R |
| 1831−00 | 520.9 | 1.8 | $< 0.004$ | 0.00012 | (0.07) | 10.9 | $6\times10^8$ | 23T |
| 1957+20 | 1.6 | 0.38[e] | $< 4\times10^{-5}$ | $5\times10^{-6}$ | 0.02[f] | 8.1 | $2\times10^9$ | 27R |
| 1257+12 | 6.2 | 67,98 | 0.02, 0.02 | 5, $3\times10^{-16}$ | 4,3 $M_\oplus$ | 8.9 | $8\times10^8$ | 28W |
| 1937+21 | 1.6 | sing. | | | | 8.6 | $2\times10^8$ | 29T |

[a] Orbital eccentricity.
[b] Mass function $f(M) = (M_2 \sin i)^3 (M_2 + M_{psr})^{-2}$.
[c] Mass of pulsar's companion (when in parentheses, tabulated value of $M_2$ is estimated from $f(M)$ assuming a pulsar mass of $1.4 M_\odot$ and inclination $i = 60°$, the median for randomly oriented binaries).
[d] B given is dipole surface field, calculated as if the pulsar were an orthogonal vacuum rotator. Higher multipoles could be much stronger.
[e] Pulsar eclipsed when behind companion (or its wind).
[f] Optical radiation from the white dwarf companion is observed; its temperature combined with the theory of white dwarf cooling confirm the age estimated from $P/(2\dot{P})$ (except for 1957+20s companion, which is heated by the pulsar's relativistic wind).

period, and can be viewed as making an impulsive change to the velocities of the stars in the binary. This induces a small eccentricity $e_f$ in the initially circular orbit:

$$e_f = \mu\lambda(a/R_p)^3 \sqrt{(3\sin^2\theta_0 + 4\cos^2\theta_0)} + O([\mu\lambda(a/R_p)^3]^2), \quad \lambda \ll 1, \tag{5.1}$$

where $\theta_0$ is the angle, at the moment of closest approach, between the line joining the two stars in the binary and the line joining the binary to the perturbing star. In this

Downloaded from rsta.royalsocietypublishing.org



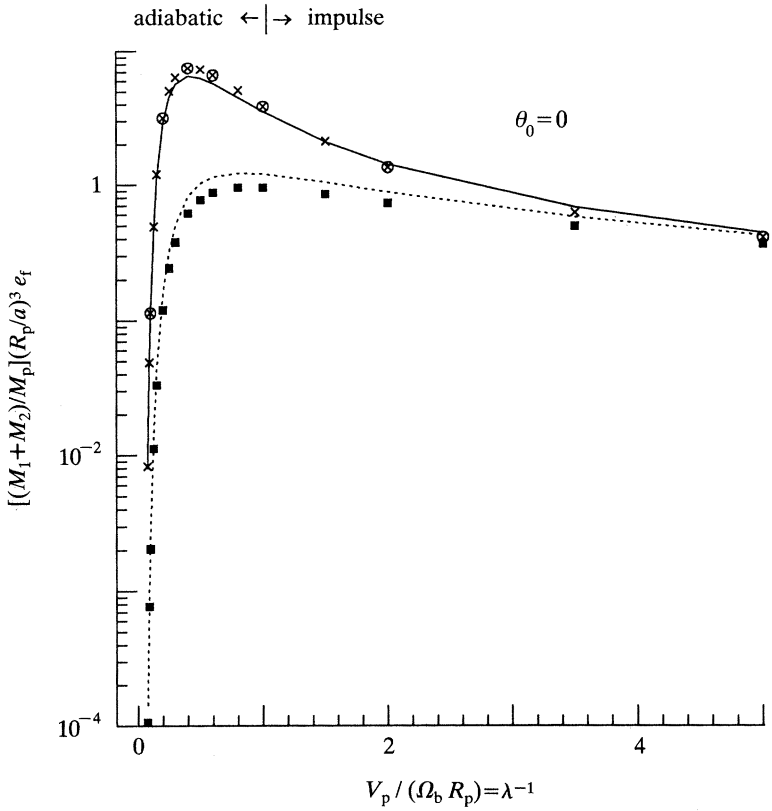


Figure 7. Eccentricity $e_f$ induced by a perturbing star $M_p$ passing at speed $V_p$ by a circular binary star system. See text for meaning of symbols. The points are the result of numerical integration. The curves are the asymptotic analytical results given in the text. ×, $R_p = 20a$, retrograde; ○, $R_p = 40a$, retrograde; ——, $[2\lambda + 6(\frac{1}{2}\pi)^{\frac{1}{2}}\lambda^{\frac{5}{2}}]\,e^{-\lambda}$; ■, $R_p = 20a$, prograde; - - - - -, $[2\lambda + (\frac{1}{2}\pi)^{\frac{1}{2}}\lambda^{\frac{3}{2}}]\,e^{-\lambda}$.

impulsive limit, the induced eccentricity is the same for prograde and retrograde encounters.

If $\lambda \gg 1$, then the encounter lasts for many orbits of the binary. The slower the encounter, the more nearly the adiabatic effects of the perturbing mass on the binary orbit average to zero. In this limit, a calculation by N. Murray (1990, personal communication) shows that the induced eccentricity is independent of $\theta_0$, but is larger for retrograde than for prograde encounters, and is given by

$$e_f = 6\mu(a/R_p)^3\,(\tfrac{1}{2}\pi)^{\frac{1}{2}}\lambda^{\frac{5}{2}}\,e^{-\lambda}, \quad \lambda \gg 1, \quad \text{retrograde}, \tag{5.2}$$

for retrograde encounters, and

$$e_f = \mu(a/R_p)^3\,(\tfrac{1}{2}\pi)^{\frac{1}{2}}\lambda^{\frac{3}{2}}\,e^{-\lambda} = (1/6\lambda)\,e_{f,\,ret}, \quad \lambda \gg 1, \quad \text{prograde}, \tag{5.3}$$

for prograde encounters when the binary and perturbing body both orbit in the same sense. Simply adding the forms of $e_f$ in the impulsive and adiabatic limits gives an excellent fit to the results of numerical integrations of the three-body problem, as shown in figure 7.

To apply these results to close binaries in globular clusters, we note that such binaries will have orbital velocities much larger than the velocity dispersion of single stars in the cluster. Thus the orbits of stars whose passages induce small eccentricities

Downloaded from rsta.royalsocietypublishing.org



are nearly parabolic, and the encounters adiabatic in the sense defined above. We make the reasonable assumptions that the $\langle e_f \rangle$ averaged over encounters from all incoming directions is approximately the geometric mean of that for prograde and retrograde encounters, and that equations (5.2), (5.3) can be extended to parabolic encounters by replacing $\lambda$ by the ratio of the binary angular velocity to that of the perturber at *pericentre*:

$$\lambda \approx [M_b/2(M_p+M_b)]^{\frac{1}{2}}(p/a)^{\frac{3}{2}}, \tag{5.4}$$

where $p$ is the separation at pericentre, and $M_b = M_1+M_2$ is the mass of the binary. Then for parabolic encounters, $e_f \approx M_p/(M_b+M_p)\exp[-\lambda]$, and we find that the approximate cross section for encounters with stars of mass $M_p$, and velocity at infinity $v_\infty$ to induce an eccentricity larger than $e_f$ is

$$\sigma(>e_f) \sim \frac{2\pi G(M_p+M_b)\,a}{v_\infty^2}\left(\frac{2(M_p+M_b)}{M_b}\right)^{\frac{1}{3}}\left[-\ln\left(e_f\frac{M_p+M_b}{M_p}\right)\right]^{\frac{2}{3}}. \tag{5.5}$$

This is in excellent agreement with the cross sections computed by Monte Carlo simulation by Rappaport *et al.* (1989, eqns 8–10), except for $e_f < 3\times10^{-3}$, where their fit gives a cross section about a factor of 2 larger, perhaps because numerical inaccuracies or premature truncation of distant flybys led them to overestimate the eccentricities induced by distant encounters. As we show in §7, however, isolated circularized binaries can have residual eccentricities this large, so observed eccentricities $< 10^{-3}$ in pulsar–white-dwarf binaries cannot unambiguously be assigned to the effects of passing stars. Cross sections at this level are thus not very interesting anyway.

Consider a globular cluster's core, where the one-dimensional velocity dispersion is $10v_{10}$ km s$^{-1}$ and the density of $M_p = 0.7M_\odot$ stars is $10^4 n_4$ pc$^{-3}$. For a $M_b = 1.6M_\odot$ binary of orbital period $P_{day}$ d, averaging the cross section (5.5) over a maxwellian velocity distribution gives a rate of encounters inducing eccentricities exceeding $e_f$

$$\langle n\sigma(>e_f)\,v_\infty\rangle = 5\times10^{-12}n_4\,v_{10}^{-1}\,P_{day}^{\frac{2}{3}}[-\ln(1.4e_f)]^{\frac{2}{3}}\,\mathrm{a}^{-1}, \tag{5.6}$$

in excellent agreement with the numerical (Monte Carlo) curves of figure 1 in Rappaport *et al.* (1989). Note that (5.6) and (5.5) apply to nearly parabolic encounters, i.e. in a typical ($v_{10} \sim 1$) globular cluster to binaries with $P_b < 10^3$ d. Encounters inducing small eccentricities in larger binaries are more nearly the straight-line encounters described by equations (5.1)–(5.3), but such binaries are soft and easily ionized (see below), and so unlikely to occur in nature.

Using equation (5.6) and the data in tables 1 and 2, we can compute the timescales $\tau_{>e} = 1/\langle n\sigma v\rangle$ on which passing stars would have given each of the cluster binary pulsars its observed orbital eccentricity. We assume that each $L_{V\odot}$ of cluster core light has two stars associated with it (lower main sequence and white dwarf stars have much mass but little light). Of particular interest are PSR1620−26 (M4: $\tau_{>0.02^5} = 10^9$ years; $P/2\dot{P} = 10^{8.3}$ years), PSR1516+02B (M5: $\tau_{>0.13} = 10^{9.7}$ years; $P/2\dot{P} > 10^9$ years) and PSR1310+18 (M53: $\tau_{>0.01} = 10^{9.8}$ years). Thus it is conceivable that these pulsars were recycled during ordinary mass transfer from a low mass giant (as suggested by their positions near the $M_c$–$P_b$ line; see §4 and figure 6), during which their orbits were accurately circularized (§7), and a passing star subsequently gave them their observed eccentricity. However, this seems quite unlikely for PSR1802−07A (NGC 6539: $\tau_{>0.21} = 10^{10.5}$ years), which the reader will recall was also unusual in lying far from the $M_c$–$P_b$ line (figure 6) for Roche

Downloaded from rsta.royalsocietypublishing.org



lobe-filling giants. Since the timescale for exchange into a binary with such a final state is considerably larger even than $\tau_{>0.21}$, this suggests that PSR1802−07A had a quite different origin, as described in §6.

### (*b*) *Exchange and ionization*

Sometimes a cluster star will happen to pass even closer to a binary, and violent interaction rather than gentle eccentricity-inducing perturbation takes place. The violent interactions can include physical collision between stars (§6), but more common are exchange of stars, hardening (increase of the binary's binding energy), and ionization (dissolution of the binary).

In this context it is useful to distinguish hard binaries (those whose binding energy $-GM_1M_2/(2a)$ exceeds the mean kinetic energy $\frac{3}{2}m_{\rm f}\sigma_{\rm f}^2$ of the single stars in the globular cluster, where $\sigma_{\rm f}$ is the one-dimensional velocity dispersion of stars of mass $m_{\rm f}$) from soft binaries (whose binding energy is less than $\frac{3}{2}m_{\rm f}\sigma_{\rm f}^2$). Analytical arguments (Heggie 1975) and numerical simulations (Hut 1983; Sigurdsson 1991) show that encounters make hard binaries harder (by $\sim 20\,\%$ per close encounter, on average), but make soft binaries softer (eventually ionizing them). This is easily understood as a consequence of the tendency to equipartition of energy and the negative specific heat of self-gravitating systems. The velocities (hence 'temperature') of the stars orbiting in a hard binary are higher than those of stars in the surrounding cluster; therefore collisions transfer energy ('heat') from the binary to the cluster. The loss of energy from the binary makes the binding energy more negative. Conversely, the stars in a soft binary have lower velocities ('temperature') than the surrounding cluster, so collisions transfer energy to the binary, making its binding energy less negative (hence eventually positive).

This thermodynamic point of view also explains another important result of numerical simulations. Namely, when the three stars involved in a close three-body encounter with a hard binary have differing masses, there is a strong tendency for the two heaviest ones to be the ones left in the final binary (Sigurdsson 1991). Thus, for example, if a neutron star or a heavy white dwarf encounters a binary containing two main sequence stars, it will preferentially be substituted for one of the lighter stars. And if a neutron star encounters another neutron star with a main sequence or giant companion (e.g. the low mass X-ray binary AC211 in M15 (Naylor *et al.* 1988)), it will nearly always eject the light companion, leaving a double neutron star binary. This, almost certainly, is how the neutron star binary PSR2127+11C formed in M15 (Phinney & Sigurdsson 1991), since the young ($10^{8.3}$ years) pulsar cannot possibly have been spun-up by its companion, degenerate for at least $10^{10}$ years!

Confirmation that this is the case comes from the recoil of exchange encounters and the position of PSR 2127+11C, 26 core radii from the centre of M15. The recoil occurs because exchanges, like all close encounters, harden a hard binary. The binding energy lost must be carried away by the escaping third star, which thus leaves with much more energy than had the incoming star. If we work in the centre-of-mass frame of the three bodies, it is evident that the momentum of this high speed escaping third star must be balanced by an equal and opposite momentum of the binary (the recoil). For most hard binaries in globular clusters, the third star will be ejected from the globular cluster altogether, but the binary, being heavier, recoils with lower velocity and so can remain bound. The distribution of recoil velocities in exchange encounters between a neutron star and a binary like AC211 ($P_{\rm b} = 8.5$ h) resulting in a double neutron star binary like PSR2127+11C are shown in figure 8.



PHILOSOPHICAL TRANSACTIONS OF THE ROYAL SOCIETY A MATHEMATICAL, PHYSICAL & ENGINEERING SCIENCES
PHILOSOPHICAL TRANSACTIONS OF THE ROYAL SOCIETY A MATHEMATICAL, PHYSICAL & ENGINEERING SCIENCES

Downloaded from rsta.royalsocietypublishing.org



Figure 8

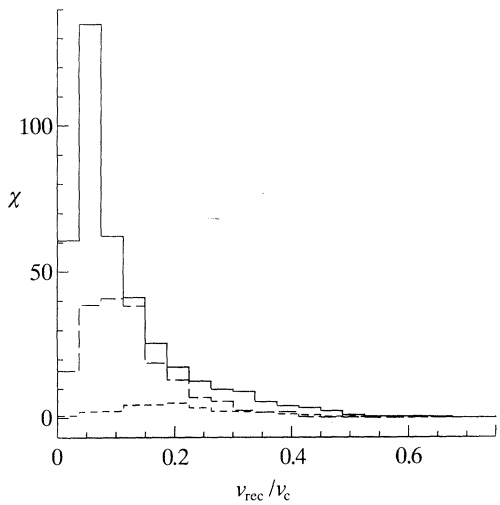


Figure 9

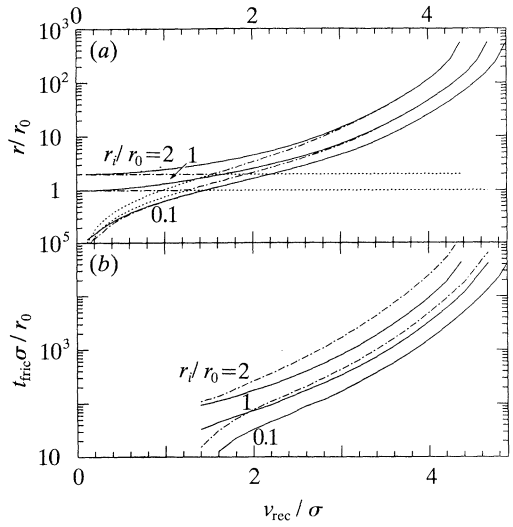


Figure 8. Differential cross sections of binary recoil velocity for flybys and exchanges in which a passing neutron star encounters a binary containing a neutron star and a $0.56M_\odot$ main sequence star ($\chi = (v_c/\pi a_{in}^2)\,(\mathrm{d}\sigma(X)/\mathrm{d}v_{rec})\,(v_{in}/v_c)^2$). The final binary consists of two stars of mass $1.0M_h$; the expelled star has mass $0.4M_h$. In the application envisaged here, $M_h = 1.4M_\odot$, appropriate for neutron stars or heavy white dwarfs. The initial binary is circular, with semi-major axis $a_i$; $v_c^2 = GM_1M_2(M_1+M_2+M_f)/(a_iM_f(M_1+M_2))$ is the relative incoming velocity for which the system would have zero total energy. $v_c = 273\ \mathrm{km\ s^{-1}}$ if the initial period $P_i = 8$ h. Note that the total cross section for heavy star exchanges which leave the light star in the binary is smaller by a factor of 6 than that which leaves the two neutron stars bound. $v_{in}/v_c \in [0.05,\ 0.15]$, ——, $X$: $(1,2)+(3)\to(1,2)+(3)$; – – – –, $X$: $(1,2)+(3)\to(1)+(2,3)$; — — — —, $X$: $(1,2)+(3)\to(1,3)+(2)$.

Figure 9. (*a*) The turning points of the orbit of a body ejected at speed $v_{rec}$ from radius $r_i$ in the core of a single-mass $W_0 = 12$ ($c = 2.74$) King model cluster of core radius $r_0$ and line-of-sight central velocity dispersion $\sigma$. The form of the curve is independent of $r_0$ and $W_0$ for $r/r_0 \ll 100$. For PSR 2127+11C to reach its projected distance of 2.7 pc from the core of M15, it must have been ejected at $\gtrsim 50\ \mathrm{km\ s^{-1}}$. (*b*) The timescale for dynamical friction to carry back to the core a star or binary system of mass $m_b$ ejected with speed $v_{rec}$ from radius $r_i$. The form of the curve is independent of $r_0$ for $r_i \gtrsim r_0$. The friction time on the ordinate is labelled for a heavy body of $10^{-5}$ the cluster mass, but scales inversely as the mass of the heavy body. (*a*) ——, Apocentre, radial recoil; — — —, apocentre, tangential recoil; – – – –, pericentre, tangential recoil. (*b*) ——, Radial recoil; — — —, tangential recoil.

About 30% of such exchanges have the $\gtrsim 50\ \mathrm{km\ s^{-1}}$ recoil required to eject the binary to its observed position in M15 (see figure 9*a*). Note that in such an exchange, there is substantial recoil even if the initial and final binaries have the same semi-major axis or orbital period, since the mass of one of the stars in the final binary and hence its binding energy, is much greater than in the initial one.

Exchange binaries are generally highly eccentric, with median $e \approx 0.7$. A rough rule of thumb for the median recoil velocity of the final binary in exchange encounters in which the lightest star $M_2$ is ejected is

$$v_{rec} \approx \frac{M_2}{2(M_1+M_f)}\sqrt{\left(\frac{G(M_1+M_f)}{a_i}\right)} = 15\frac{M_2}{(M_1+M_f)^{\frac{1}{2}}}a_{AU}^{-\frac{1}{2}}\ \mathrm{km\ s^{-1}}, \qquad (5.7)$$

where $a_i = a_{AU}$ A.U. is the semi-major axis of the pre-encounter binary, and in the



PHILOSOPHICAL TRANSACTIONS OF THE ROYAL SOCIETY A MATHEMATICAL, PHYSICAL & ENGINEERING SCIENCES
PHILOSOPHICAL TRANSACTIONS OF THE ROYAL SOCIETY A MATHEMATICAL, PHYSICAL & ENGINEERING SCIENCES

Downloaded from rsta.royalsocietypublishing.org



second equality the masses are in solar units. Thus recoil in exchanges into binaries with $a < 0.1$ A.U. are sufficient to send the binaries into orbits extending well outside the core of a globular cluster.

Once ejected, the binary (being heavier than the mean stellar mass in the cluster) is dragged by dynamical friction back to the core of the cluster. After ejection, the binary's orbit in the cluster is very elongated, with pericentre near the point of ejection (almost always in the dense core). The friction time, shown in figure 9*b* (which, but for a printing error, would have been figure 1 of Phinney & Sigurdsson (1991)), is determined largely by the density at pericentre. Perpendicular velocity kicks from cluster stars passing on the outer reaches of the orbit can shift the pericentre of the nearly radial orbit of the ejected body, creating a distribution of sinking times with a tail extending to times much larger than indicated by the curve, which neglects such kicks. The width of this distribution of sinking times becomes significant for orbits with initial apocentric distances $r_a$ more than $4(M_b + \langle m \rangle)/\langle m \rangle$ times the initial pericentric distance, where $\langle m \rangle$ is the mean mass of cluster stars encountered near $r_a$. The timescale for the binary pulsar 2127+11C to sink within M15 is $\sim 10^8 (r_p/0.1\ \mathrm{pc})$ years, comparable with both its characteristic age and its lifetime against gravitational radiation. The timescale for the binary pulsar 1744−24A to sink within Terzan 5 is $\gtrsim 1 \times 10^8$ years. Neither system's pericentric distance is likely to have been shifted substantially. Ejected pulsars are most likely to be found near the half-mass radius (3.5 pc for M15): convolution of figure 9*a* and 8 shows that few pulsars will be found beyond the half-mass radius ($32 r_0$), since only a very narrow range of ejection velocities have apocentres there. Few will be found inside the half-mass radius, since friction will there rapidly drag them back to the core.

## 6. Pulsars in globular star clusters

Globular clusters are 10–20 Ga old, and contain no interstellar medium from which stars could form, nor can they capture stars from the Galaxy. Thus the most massive single star on the main sequence has $M \approx 0.8 M_\odot$. Neutron stars, and young pulsars, are believed to be formed in supernova explosions of $\gtrsim 10 M_\odot$ stars. Hence there should be no pulsars with characteristic ages much less than $10^{10}$ years in globular clusters. Table 1 shows that there are many. These relatively young pulsars must then either be old neutron stars recently spun back up to short periods by accretion, or be neutron stars created recently by accretion-induced collapse (AIC) of a massive white dwarf. In either case, the formation of the pulsar must have been preceded by a phase of accretion onto a neutron star. Accreting neutron stars appear as X-ray sources. There is consequently a close connection between X-ray burst sources and pulsars in globular clusters.

In globular clusters, X-ray burst sources and recycled pulsars are roughly 100 times more abundant per unit mass than in the Galactic disc (Johnston *et al.* 1992). It is quite out of the question that neutron stars be 100 times more abundant in globular clusters; in fact §2 suggests that their abundance is about the same as in the Galaxy. Thus somehow neutron stars (or heavy white dwarfs suitable for AIC) in globular clusters must be 100 times more likely to end up accreting, i.e. they must capture their own binary companions. The high density of stars in globular clusters suggests several possible capture routes.

Hills (1976) first proposed the idea that exchanges with primordial binaries in dense stellar systems would lead to an unusually large population of compact objects



PHILOSOPHICAL TRANSACTIONS OF THE ROYAL SOCIETY A MATHEMATICAL, PHYSICAL & ENGINEERING SCIENCES
PHILOSOPHICAL TRANSACTIONS OF THE ROYAL SOCIETY A MATHEMATICAL, PHYSICAL & ENGINEERING SCIENCES

Downloaded from rsta.royalsocietypublishing.org



in binaries. However, the failure of Gunn & Griffin (1979) to detect a single binary in their radial velocity survey of M3 led most theorists to assume that there were no primordial binaries in globular clusters. In the absence of primordial binaries, the only way for a single neutron star to collect matter to accrete (to make an X-ray source, or to spin up a dead pulsar) was through tidal capture (Fabian *et al.* 1975; McMillan *et al.* 1987; Verbunt *et al.* 1987).

The rate at which neutron stars in a globular cluster of central velocity dispersion $10\sigma_{10}$ km s$^{-1}$ tidally capture companions is

$$\mathscr{R}_{\mathrm{T2}} = 7\times10^{-8}\ \mathrm{a}^{-1}\,\frac{\rho_{\mathrm{V}}}{10^6 L_{\odot\mathrm{V}}\ \mathrm{pc}^{-3}}\,\sigma_{10}^{-1.14}\,\frac{N_{\mathrm{ns}}}{10^3}, \tag{6.1}$$

proportional to the number of neutron stars and the density of ordinary stars in the cluster core. Since all globular clusters have about the same mass, and hence presumably about the same number of neutron stars, the rate of tidal capture should scale as the central density of the globular cluster. The rate (6.1) seems adequate to explain the several $\sim 10^8$ year-old pulsars in the dense globular cluster M15 (table 1). All but two of the twelve X-ray sources in globular clusters are found in clusters of the highest central densities (Predehl *et al.* 1991), consistent with the scaling with cluster density expected if all of them had formed by tidal capture.

Thus it was a considerable surprise that even very low density clusters such as M13 and M3 (see table 1) should be found to contain pulsars at almost the same rate as 100 to 1000-times denser clusters (Johnston *et al.* 1992). These evidently cannot be forming by tidal capture. At about the same time, however, primordial binaries were discovered in globular clusters (Pryor *et al.* 1989). This led to a reconsideration of Hill's (1976) suggestion that exchange into primordial binaries could be responsible for some of the pulsar recycling. This process is particularly important for neutron stars, whose apparently large velocities at birth would eject them from most binaries. Thus, while white dwarfs might exist in primordial binaries, few neutron stars are likely to (galactic pulsar statistics suggests that fewer than 1 in $10^3$ are recycled in binaries). A few exchanges can thus have a significant effect on the number of neutron stars in binary systems.

The cross section for exchange into a binary of semi-major axis $a = a_{\mathrm{AU}}$ A.U. is $\sim 100 a_{\mathrm{AU}}$ times the two-body tidal capture cross section. The relative rates of exchange and tidal capture thus depend on the fraction of binary stars in the cluster core (where should lie most of the neutron stars; see §5), and on the semi-major axes of those binaries. Binaries, being heavy, will initially tend to sink to the core of a globular cluster. Thus the binary fraction in the core can be substantially higher than the cluster-averaged fraction of $\sim 10\%$ (Pryor *et al.* 1989). Even allowing for ionization of very wide binaries (§5), a distribution of binary semi-major axes similar to the galactic one would then lead to a rate of exchange of neutron stars into binaries some 10–30 times the rate of two-body tidal capture. The locations of the binary pulsars in the globular clusters M53, M4, M5, 47 Tuc (E), and M13 near the core-mass period relation for Roche lobe overflow (figure 6) suggests that they may have formed in this way.

In globular clusters with core luminosity densities exceeding

$$\rho_{\mathrm{V}} > 1.5\times10^3 L_{\odot\mathrm{V}}\ \mathrm{pc}^{-3}\,a_{\mathrm{AU}}^{-1}\,\sigma_{10}, \tag{6.2}$$

primordial binaries with semi-major axes greater than $a$ will typically have undergone encounters with other stars intimate enough to have exchanged stars or



PHILOSOPHICAL TRANSACTIONS OF THE ROYAL SOCIETY A MATHEMATICAL, PHYSICAL & ENGINEERING SCIENCES
PHILOSOPHICAL TRANSACTIONS OF THE ROYAL SOCIETY A MATHEMATICAL, PHYSICAL & ENGINEERING SCIENCES

Downloaded from rsta.royalsocietypublishing.org



changed the orbital parameters of the binary significantly. In such clusters, therefore, the population of binaries with orbital periods longer than $P_b \sim$ years will no longer be truly 'primordial', but its stellar composition, and semi-major axis and eccentricity distributions will be determined in large part by past interactions with field stars and other binaries. Numerical simulations (Gao *et al.* 1991; Heggie & Aarseth 1992) show that during the initial gravothermal collapse of a cluster's core, the central density increases so rapidly that the binaries do not have time to be significantly hardened. Thus $\langle n\sigma v\rangle$ for binary-hardening encounters increases, until enough energy is being released by these encounters to halt core collapse (which was caused in the first place by the conduction of kinetic energy from the core of the cluster to the edges of the cluster kept 'cold' by escape of stars). The cluster then remains at a roughly constant central density $\sim 10^5\, M_\odot\ \mathrm{pc}^{-3}$, 'burning' its binaries until so many of them have been ejected by recoil (§5) that they can no longer supply the energy needed to prevent further core collapse. Clusters at the onset of the 'binary burning' phase of their lives should have the largest total rate of binary encounters, and a potentially enormous rate of pulsar recycling. The clusters 47 Tuc and Ter 5 both have short apparent collapse times, suggesting that they are in such a phase. This may explain the extraordinarily large number of bright pulsars and pulsar-like radio sources they respectively contain.

As described in §5, exchanges typically remove only a small fraction $\lesssim 25\,\%$ of a binary's binding energy, and typically lead to ejection of the lightest star. Thus exchanging a light main sequence star $M_2$ or white dwarf for a neutron star $M_p$ in a binary means that the final semi-major axis is larger than the initial one by a factor $\sim M_p/M_2 > 1$. This increases the binary's cross section for subsequent close encounters. Many exchanges are not simple single-pass events, but are complicated resonant interactions like the one shown in figure 10. It is not surprising that during the many passes the three stars make at each other during such an encounter, there is a substantial probability for a tidal or direct collision. Thus a large fraction of all close encounters between binaries lead to tidal capture or collisions. Since binaries can be hundreds of times bigger than the individual stars, this means that a population of stars in binaries will have a much higher rate of tidal captures and collisions than the same population of stars at the same density would have if all the stars were single. This three-body tidal capture cross section

$$\sigma_{T3} \approx 5(a/R)^{1-\gamma}\,\sigma_{T2}. \tag{6.3}$$

The exponent $1-\gamma \approx 0.3$ when the stars (one or two of which have radius $R > 10^{-3}\,a$) all have masses comparable within a factor of three and $v_\infty < 0.5\,v_c$ (Sigurdsson 1991).

In about half of all three-body encounters leading to collisions, the bystander star is unbound from the merged collision product. If the neutron stars accretes some of the collisional debris (cf. Krolik *et al.* 1984), this is then a mechanism for making isolated recycled pulsars in globular clusters (Verbunt *et al.* 1987). This is also an attractive way to explain the X-ray source in the low density globular cluster NGC 6712. The optical counterpart of this X-ray source has $M_V \approx 5.6$ (Aurière & Koch-Miramond 1991), much fainter than a giant or subgiant, and nearly 100 times fainter than the average low-mass X-ray binary (Van Paradijs 1983), suggesting that it did not form by exchange followed by ordinary nuclear evolution of the companion. Yet ordinary tidal capture of a main sequence star is quite improbable (though not entirely out of the question, given that only 1 in $\sim 50$ low density clusters contain X-ray binaries).



PHILOSOPHICAL TRANSACTIONS OF THE ROYAL SOCIETY A MATHEMATICAL, PHYSICAL & ENGINEERING SCIENCES
PHILOSOPHICAL TRANSACTIONS OF THE ROYAL SOCIETY A MATHEMATICAL, PHYSICAL & ENGINEERING SCIENCES

Downloaded from rsta.royalsocietypublishing.org



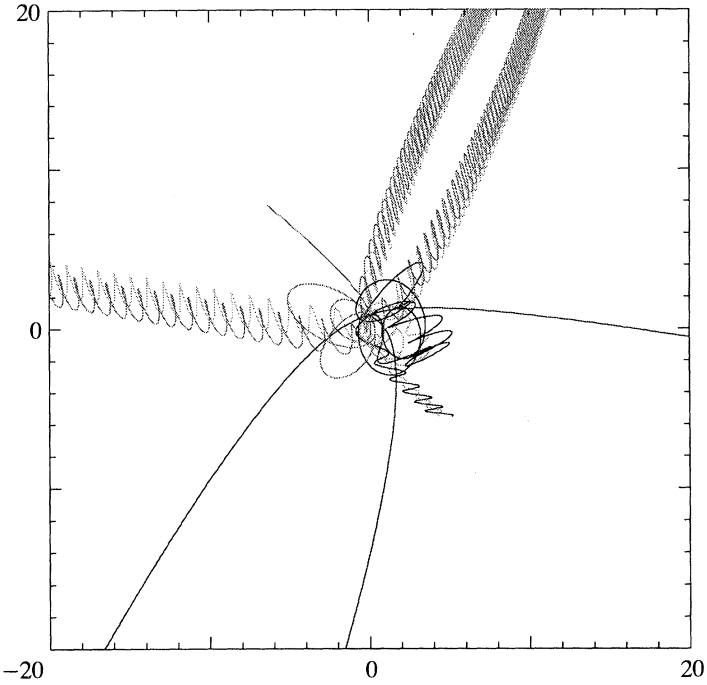


Figure 10. A resonant three-body encounter. A neutron star (heavy line) is incident from the right on a binary containing two main sequence stars (spirals on the left). After several close passages, the lighter of the two main sequence stars is ejected toward the upper left and the binary, now containing the neutron star, recoils in the opposite direction. If the initial orbit (scale-free in this point-mass simulation) has been smaller than 0.5 A.U., the neutron star would have collided with the lighter of the main sequence stars during the encounter.

In the other half of the collisional three-body encounters, however, the bystander star remains bound in a highly eccentric orbit to the collision product. Tidal dissipation (§7) subsequently reduces the orbital period and eccentricity of the bystander. If the collision product becomes a recycled pulsar, this is then a mechanism for making recycled pulsars in short-period eccentric binaries, such as PSR1802−07A in NGC 6539.

## 7. Residual eccentricities of tidally circularized orbits

The orbits of Galactic pulsars in binary systems are not circular. Our interest here is in the Galactic pulsars with companions of low mass, $0.2$–$0.5 M_\odot$. These have small, but measurably non-zero eccentricities, ranging from $\sim 10^{-2}$ to $\sim 10^{-5}$ (see the third group of entries in table 3).

Immediately after the neutron star formed, these orbits must have been much more eccentric. If the neutron star formed in a supernova explosion, the associated large impulsive mass loss virtually guarantees a highly eccentric orbit. In fact, the binary system would become unbound if the exploding star had not previously lost its hydrogen envelope, or the explosion were not asymmetrical in a suitably contrived direction and amount. This is seemingly confirmed by the orbits of the pulsars with neutron star companions, PSRs 1913+16, 2303+46 and 1534+12,

Downloaded from rsta.royalsocietypublishing.org



which respectively have eccentricities of 0.62, 0.66, and 0.27. Even were the neutron star to form without loss of baryons, in the collapse of a white dwarf driven by accretion beyond its maximum stable mass, the initial orbital eccentricity $e$ would exceed $\sim 0.1$. This is because neutrinos carry off the binding energy of the final neutron star, reducing the gravitational mass of the system by $\sim 0.2 M_\odot$ in a time much shorter than the orbital period. In either case, the orbits of the pulsars in all but the first group table 3 must have been circularized after their neutron stars formed. The next paragraph explains (cf. the elegant series of papers by Zahn (1966)) how this circularization occurred. The remainder of the section addresses the question of why the eccentricities are not consequently much smaller than they are observed to be.

Some time after the neutron star (now the pulsar) forms, its companion's nuclear evolution will cause the companion to swell to a giant, as described in §4. As it swells, it will become more and more distorted by the gradient of the pulsar's gravitational field. If the orbit is eccentric, the tide, and hence the companion's tidal distortion, will be time dependent. The energy so dissipated comes from the energy of epicyclic motion of the eccentric orbit, which, like the dissipation, vanishes for a circular orbit. Thus the dissipation inexorably leads to damping of the epicyclic motion and so circularizes the orbit (the tide is also time dependent if the companion's rotation period is not equal to the orbital period. It can be shown, however, that the tidal torque synchronizes the spin even faster than it damps the orbital eccentricity, so the late stages of evolution are well described as circularization of an orbit with the companion locked in synchronous rotation. A neutron star, by contrast, is so tiny that tidal forces on it are utterly negligible, so pulsar spins are not synchronized).

### (*a*) *Tidal circularization*

Consider a nearly circular binary of semi-major axis $a$, period $P_\mathrm{b}$, and eccentricity $e \ll 1$. The tidal forces caused by the pulsar, of mass $M_\mathrm{p}$, on its synchronous swollen companion, of mass $M_\mathrm{c}$ and radius $R_\mathrm{c}$ can be decomposed into a static tide and a variable tide. The static tide distorts the equipotential of the companion's surface from the sphere it would be in isolation by a height $\sim (M_\mathrm{p}/M_\mathrm{c})\,(R_\mathrm{c}^4/a^3)$, but since it is static, causes no motion or dissipation in the companion. The variable tide is most easily understood from the point of view of an observer standing on the surface of the companion with the pulsar initially overhead. Over the course of an orbit, he would see the pulsar's distance vary by $\pm ae$. After one orbit, the pulsar would again be overhead. But Kepler's second law requires that the orbital angular velocity vary as the inverse square of the pulsar distance, while the companion rotates at constant angular velocity $2\pi/P_\mathrm{b}$ (as synchronous as it can be). So the pulsar will in the interval have wandered back and forth by an angle $\sim e$ across the observer's sky. Thus the variable tide gives both vertical and horizontal displacements of amplitude

$$\xi \sim (M_\mathrm{p}/M_\mathrm{c})\,(r^4/a^3)\,e, \tag{7.1}$$

at radius $r$ from the centre of the companion (assumed centrally concentrated enough that $M(<r) \approx M_\mathrm{c}$). Since $\xi$ varies at the orbital frequency $\Omega_\mathrm{b} = 2\pi/P_\mathrm{b}$, material near the companion's surface must move with velocity $u \sim \Omega_\mathrm{b}\,\xi$, and have both vertical and horizontal velocity gradients

$$\nabla u \sim \Omega_\mathrm{b}\,\xi/r. \tag{7.2}$$

Let us temporarily pretend that there is a non-zero viscosity $\nu$ only in a layer of the

Downloaded from rsta.royalsocietypublishing.org



star of thickness $H$ and density $\rho$, at radius $r$ ($< R_c$) within the companion. Then the rate of viscous dissipation of energy in the motion driven by the variable tide is

$$\dot{E}_{\rm diss} \approx 4\pi r^2 H \rho \nu |\nabla u|^2. \tag{7.3}$$

If the companion is convective at the surface, the largest viscosity will be eddy viscosity,

$$\nu = \nu_{\rm eddy} \sim H v_H, \tag{7.4}$$

where $v_H$ is the velocity of convective motion in the eddies of scale height $H$. Combining the last four equations, we have

$$\dot{E}_{\rm diss} \approx 4\pi \rho v_H H^2 \Omega_{\rm b}^2 (M_{\rm p}/M_{\rm c})^2 (r^8/a^6)\, e^2. \tag{7.5}$$

This comes at the expense of the epicyclic energy of the orbit. This is the difference in total energy between the eccentric orbit and a circular orbit of the same angular momentum (nearly conserved in the evolution):

$$E_{\rm e} = \tfrac{1}{2} G M_{\rm p} M_{\rm c}\, e^2/a. \tag{7.6}$$

Equating $\mathrm{d}E_{\rm e}/\mathrm{d}t = -\dot{E}_{\rm diss}$ and using $\Omega_{\rm b}^2 = G(M_{\rm c}+M_{\rm p})\, a^{-3}$ in the last two equations, we see that the eccentricity decays exponentially,

$$e(t) = e(0) \exp\left[ -\int_0^t \mathrm{d}t'/\tau_{\rm c}(t') \right], \tag{7.7}$$

where the circularization timescale $\tau_{\rm c}$ is given by

$$\frac{1}{\tau_{\rm c}} = -\frac{1}{e}\frac{\mathrm{d}e}{\mathrm{d}t} = \frac{8\pi\rho H^3}{M_{\rm c}} \frac{v_H}{H} \frac{M_{\rm c}+M_{\rm p}}{M_{\rm p}} \left(\frac{M_{\rm p}}{M_{\rm c}}\right)^2 \left(\frac{r}{a}\right)^8. \tag{7.8}$$

In a convective layer of a star of luminosity $L$, the flux $F = L/(4\pi r^2)$ is carried by convection, $F \sim \rho v_H^3$. Thus the eddy turnover frequency

$$\frac{1}{\tau_{\rm eddy}} \sim \frac{v_H}{H} \sim \left(\frac{L}{4\pi r^2 \rho H^3}\right)^{\frac{1}{3}}. \tag{7.9}$$

Substituting this in equation (7.8), we have

$$\frac{1}{\tau_{\rm c}} = -\frac{1}{e}\frac{\mathrm{d}e}{\mathrm{d}t} = \left(\frac{L}{M_{\rm la} r^2}\right)^{\frac{1}{3}} \left(\frac{H}{r}\right)^{\frac{4}{3}} \frac{2M_{\rm la}}{M_{\rm c}} \frac{M_{\rm c}+M_{\rm p}}{M_{\rm p}} \left(\frac{M_{\rm p}}{M_{\rm c}}\right)^2 \left(\frac{r}{a}\right)^8, \tag{7.10}$$

where $M_{\rm la} = 4\pi\rho r^2 H$ is the mass of the viscous layer.

To calculate the circularization rate for a red giant star, we must sum equation (7.10) over all the convective layers of the giant. Convection keeps the giant's envelope isentropic, so outside of ionization zones, $p \propto \rho^{\frac{5}{3}}$. Thus for (surface) layers at $r > \frac{1}{2}R_{\rm c}$, the density scale height $H \sim (R-r)$, $\rho \propto H^{\frac{3}{2}}$, $M_{\rm la} \propto H^{\frac{5}{2}}$, and the layer's contribution to $1/\tau_{\rm c} \propto H^{\frac{22}{9}}$. Thus the deepest of these layers have most of the mass and damping. For the deep layers at $r < \frac{1}{2}R_{\rm c}$, $H \sim r$, $\rho \propto r^{-\frac{3}{2}}$, $M_{\rm la} \propto r^{\frac{3}{2}}$, and the layer's contribution to $1/\tau_{\rm c} \propto r^{\frac{25}{3}}$. Therefore in a red giant, most of the envelope's mass and damping arise from the convection cells at $r \sim \frac{1}{2}R_{\rm c}$, with scale height of order their radii. Thus to a very good approximation (confirmed by more careful integrations over giant structure)

$$\frac{1}{\tau_{\rm c}} = -\frac{1}{e}\frac{\mathrm{d}e}{\mathrm{d}t} = f\left(\frac{L}{M_{\rm env} R_{\rm c}^2}\right)^{\frac{1}{3}} \frac{M_{\rm env}}{M_{\rm c}} \frac{M_{\rm c}+M_{\rm p}}{M_{\rm p}} \left(\frac{M_{\rm p}}{M_{\rm c}}\right)^2 \left(\frac{R_{\rm c}}{a}\right)^8, \tag{7.11}$$

Downloaded from rsta.royalsocietypublishing.org



where $f$ is a dimensionless number of order unity which depends on the mixing length parameter, the coefficient of turbulent viscosity, and (very weakly) on the density profile of the giant's envelope. This equation (with $f = 0.8$) was derived by Zahn (1977), as corrected in 1978 in an erratum; a nicely pedagogical discussion of the physics is in Zahn (1966)), except that he assumed $M_{\rm env} = M_{\rm c}$, appropriate for detached giants but not for those for which mass transfer has reduced $M_{\rm env} \ll M_{\rm c}$.

### (*b*) *Testing tidal circularization theory*

Since $f$ in equation (7.11) for the rate of tidal circularization depends on mixing lengths and the coefficient of eddy viscosity, whose precise numerical values are the subject of some controversy, it seemed desirable to subject the circularization theory to a quantitative test, and so check the scalings with $R_{\rm c}$, $M_{\rm c}$, etc., and constrain $f$.

The populations of spectroscopic binaries in open star clusters are ideal for this purpose. All the giant and subgiant stars in a given cluster have nearly the same mass, and since that mass and the cluster's distance can be determined by main sequence fitting (if not by more direct means), multicolour photometry can determine $L$, $T_{\rm eff}$, and hence $R_{\rm c}$ for each star. The binaries of interest are those containing a giant (or subgiant) of mass $M_{\rm c}$ and a main sequence star (pointlike mass $M_{\rm p}$, here playing the role of what in deriving equation (7.11) we call the pulsar). If the spectroscopic binary is double-lined, $M_{\rm p}$ can be determined directly; if not, it can be estimated statistically from the mass function. The orbital period, total mass, and Kepler's third law determine the orbital semi-major axis $a$. Thus all quantities on the right-hand side of equation (7.11) except $f$ are determined directly from observables.

Consider now the evolution of an eccentric binary wide enough that when both stars are on the main sequence, $\tau_{\rm c}$ exceeds the main sequence lifetime of the more massive star. Then when that star (mass $M_{\rm c}$) begins to evolve off the main sequence, the binary will still have its primordial eccentricity (median $e(0) \approx 0.3$). As the star swells, the rate of circularization $1/\tau_{\rm c}$ (equation (7.11)) increases rapidly: by a factor of $\sim 10^8$ for each factor of 10 increase in $R_{\rm c}$ (the factor $(L/R_{\rm c}^2)^{\frac{4}{3}} \propto T_{\rm eff}^{\frac{4}{3}}$ is nearly constant as a star ascends the giant branch), and

$$-\Delta \ln e = \int_0^t {\rm d}t'/\tau_{\rm c}(t')$$

(see equation (7.7)) starts to exceed unity. When it exceeds 3, the eccentricity of a median binary will have been reduced to a (spectroscopically) undetectable 0.01.

Verbunt & Phinney (1992) have integrated equation (7.11) along the evolutionary tracks appropriate to 31 binaries in 12 open clusters. Using these tracks and the observationally determined parameters, they find that binaries for which (7.11) predicts $(-\Delta \ln e)/f > 3$ are circular, while those with predicted $(-\Delta \ln e)/f < 3$ have large eccentricities. This constrains $f$: $0.5 \lesssim f \lesssim 2$, as predicted by simple theory. It also holds over a wide range of $R_{\rm c}$ and $a$, and confirms that the circularization depends on $(R_{\rm c}/a)$ as predicted.

(Some care is required to distinguish binaries: (1) in which the companion is a white dwarf, whose previous evolution can have circularized the orbit even if the presently observed giant cannot have, and (2) those in which the giant is actually a He core burning 'red clump' star, which during hydrogen shell burning previously reached a maximum radius much larger than its current one.)

Downloaded from rsta.royalsocietypublishing.org



### (c) *The puzzle*

As the giant continues to swell and mass transfer begins, the predicted $-\Delta \ln e$ continues to rise, easily reaching values of $10^2$–$10^4$. The puzzle is then the following: the pulsars with low mass white dwarf companions (third group in table 3) must, as described in §4, have been through a phase in which the red giant progenitor of the white dwarf filled its Roche lobe ($R_c \gtrsim 0.25a$). Unless the mass transfer was dynamically unstable (a possibility for PSR0655+64 (see §4 and figure 6), but very unlikely for the three millisecond pulsars in the third group of table 3, whose spin-up would need at least $\sim 10^6$ years even at the Eddington accretion rate), the circularization theory outlined above then predicts orbital eccentricities less than $e^{-100}$ ($10^{-43}$). The observed eccentricities while small, are definitely non-zero and range from $10^{-5}$ to $10^{-2}$. So, although many authors have happily pointed out that the orbits of these pulsars are nearly circular, confirming that circularization took place 'as predicted', the orbits are in fact tens of orders of magnitude more eccentric than the standard theory of tidal circularization would predict. This puzzle seems not to have been noticed before.

Before recognizing the ineluctable consequence for tidal circularization of the fluctuation–dissipation theorem (described in the next subsection), I considered a number of other mechanisms which would impart eccentricities to circularized orbits. All seem unimportant. Perturbations to the binary by passing stars can induce eccentricities given by equations (5.1)–(5.3). However, the probability that passing disc or halo stars (or putative $10^6 M_\odot$ black holes making up dark matter in the galactic halo) would pass close enough to any one of the pulsars to excite its observed eccentricity is small, and the probability that all four pulsars in the third group of table 3 should have had such close passages is incredible. Small eccentricities can also be induced by rapid mass loss at the end of the red giant's evolution. However, to produce the observed eccentricities would require terminal mass loss rates $\dot{M} \gtrsim 10^{-2} M_\odot\ \mathrm{a}^{-1}$, and the other pulsars require even larger rates. Finally, the accretion disc around the neutron star is non-axisymmetric and torques could cause growth of the orbital eccentricity. However, unless the disc's viscosity parameter $\alpha$ is much smaller than expected ($\alpha < 10^{-6}$, compared with $\alpha \sim 10^{-2}$–1 favoured by models of outbursts in cataclysmic variables), the disc mass is so low that eccentricities as large as those observed appear unattainable.

By contrast, resonant excitation of the massive circumbinary discs which might exist around protostars can pump large eccentricities on interesting timescales. This has been proposed as the mechanism for giving binary stars their large primordial eccentricities (Artymowicz *et al.* 1991).

### (d) *Convection, fluctuation–dissipation, and residual eccentricities*

The epicyclic motion of a binary in a slightly eccentric orbit can be viewed as a harmonic oscillation about the guiding circular orbit. If one of the stars is large and convective, this oscillation is, as described above, damped by the turbulent viscosity of eddies mixing its momentum. The simplest familiar example of a damped harmonic oscillator is a pendulum swinging in air. As the pendulum swings, it collides preferentially with air molecules on its leading side, thus losing energy until seemingly at rest. We all know, however, that the pendulum is never really at rest; if it were, bombardment by air molecules would gradually, and randomly increase its momentum and energy. The actual energy is then a random variable. But the mean



PHILOSOPHICAL TRANSACTIONS OF THE ROYAL SOCIETY A MATHEMATICAL, PHYSICAL & ENGINEERING SCIENCES
PHILOSOPHICAL TRANSACTIONS OF THE ROYAL SOCIETY A MATHEMATICAL, PHYSICAL & ENGINEERING SCIENCES

Downloaded from rsta.royalsocietypublishing.org



energy, for which the drag and the brownian excitation balance, is given by the familiar equipartition theorem of statistical mechanics: $\frac{1}{2}kT$ per harmonic degree of freedom. Hence $\langle E_{\rm pend}\rangle = kT_{\rm air}$. Roughly, a pendulum's (statistical) minimum energy is equal to that of a single air molecule.

What in the tidally circularizing binary are the analogues of the air molecules and $kT_{\rm air}$? One might guess that they are the convective eddies and their kinetic energy. We now show that this guess is correct, and that it offers a quantitative explanation of the eccentricities observed in the pulsar binaries.

The coupling between convective eddies and the epicyclic motion (the analogues of the collisions between air molecules and the pendulum) is through the density fluctuations produced by convection. Convection occurs because heated fluid elements expand ($\delta\rho/\rho = -\delta T/T < 0$) and rise buoyantly for about one density scale height $H = (-\mathrm{d}\ln\rho/\mathrm{d}r)^{-1}$. While rising, they reach terminal speed $v_H$ given by

$$v_H^2 \approx g(\delta\rho/\rho)H \approx c_{\rm s}^2\langle\delta\rho^2\rangle^{\frac{1}{2}}/\rho, \tag{7.12}$$

where $c_{\rm s}$ is the local sound speed. In the mixing length picture, these rising fluid elements transfer their energy to eddies at the next scale height, and, having so cooled and become denser, sink back down. The thermal and kinetic energy fluxes in the eddies, both of order $\rho v_H^3$, carry most of the star's luminosity, so $v_H$ is determined by

$$L/4\pi r^2 \approx \rho v_H^3. \tag{7.13}$$

Models of red giant envelopes give us $\rho(r)$, $c_{\rm s}(r)$, and $L(r)$, so equations (7.12) and (7.13) (which, up to numerical coefficients of order unity, describe standard mixing length theory outside of ionization or partly radiative zones) determine the scale ($\sim H$) and rms amplitude $\langle\delta\rho^2\rangle^{\frac{1}{2}}/\rho$ of density fluctuations at each point in the star. The density field of these eddies fluctuates randomly, with decorrelation time given by equation (7.9). This causes the star's external gravitational force field to fluctuate; these fluctuating forces acting on the pulsar are what excites the orbital eccentricity. Conservation of mass and linear momentum keep the star's monopole and dipole moments fixed. The quadrupole moment tensor

$$Q_{ij} = \int (3x_i x_j - r^2\delta_{ij})\,\rho(\boldsymbol{x})\,\mathrm{d}^3x \tag{7.14}$$

is the lowest fluctuating moment, and the one which dominates the fluctuating force at large distances.

Just as we did in our calculation of tidal dissipation, let us now temporarily pretend that the convection is confined to a layer of scale height $H$ at radius $r$. The contribution $\delta(\delta Q_{zz})$ of one convective eddy to the fluctuation $\delta Q_{zz}$ of e.g. $Q_{zz}$ is the difference between the value of $Q_{zz}$ in the presence of the eddy (whose temperature and density profile must be rather step function-like, as in Bénard convection cells) and the smooth averaged density profile. Thus

$$\delta(\delta Q_{zz}) \approx (3\cos^2\theta - 1)\,\rho H^4 r\,\delta\rho/\rho, \tag{7.15}$$

where $\theta$ is the polar angle between the eddy and the $z$-axis, and we have assumed that the eddy covers area $\sim H^2$. There are $N \approx 4\pi r^2/H^2$ such eddies in the layer, and in each eddy $\delta\rho/\rho$ is an independent random variable. Thus $\langle\delta Q_{zz}\rangle = 0$, but the variance, integrated over the layer at radius $r$ is non-zero:

$$\langle(\delta Q_{zz})^2\rangle \approx N[\delta(\delta Q_{zz})]^2 \simeq N\tfrac{4}{5}H^8 r^2\rho^2\langle\delta\rho^2\rangle/\rho^2, \tag{7.16}$$

so the r.m.s. fluctuating quadrupole moment contributed by the layer is

$$\langle(\delta Q_{zz})^2\rangle^{\frac{1}{2}} \approx H^3 r^2\rho\,\langle\delta\rho^2\rangle^{\frac{1}{2}}/\rho. \tag{7.17}$$



PHILOSOPHICAL TRANSACTIONS OF THE ROYAL SOCIETY A MATHEMATICAL, PHYSICAL & ENGINEERING SCIENCES

Downloaded from rsta.royalsocietypublishing.org



Because of this fluctuating quadrupole, the neutron star at distance $|\boldsymbol{x}|$ from the centre of the companion, moves through a fluctuating potential

$$\delta\phi = \frac{1}{2}\sum_{i,j}\frac{G\delta Q_{ij}\,x_i\,x_j}{|\boldsymbol{x}|^5}, \tag{7.18}$$

and thus feels fluctuating forces $\delta F(t)$ of order

$$\delta F(t) \sim \delta Q_{ij}\,GM_{\rm p}/a^4. \tag{7.19}$$

The equation for the radial motion $x = r - r_0$ of the eccentric orbit with guiding circle radius $r_0 \approx a$ is then

$$\mu\ddot{x} + (\mu/\tau_{\rm c})\,\dot{x} + \mu\Omega_{\rm b}^2\,x = \delta F(t), \tag{7.20}$$

where $\mu = M_{\rm p}\,M_{\rm c}/(M_{\rm p}+M_{\rm c})$ is the reduced mass, $\Omega_{\rm b}^2 = G(M_{\rm p}+M_{\rm c})\,a^{-3}$ is the square of the orbital frequency, and $\tau_{\rm c}$ is the circularization timescale (given, in the case of a single convective layer by equation (7.8), and in general by equation (7.11)). The left-hand side of equation (7.20) describes slowly damped (since $1/\tau_{\rm c} \ll \Omega_{\rm b}$) harmonic oscillations of amplitude $ae$ in $x = r - r_0$. The right-hand side is the random forcing term, with rms amplitude given by equations (7.19) and (7.17), and decorrelation time given by equation (7.9).

To solve the stochastic differential equation (7.20), we define power spectral densities for the fluctuating force and the epicyclic radius:

$$\left.\begin{aligned} f(\omega) &= \frac{2}{\pi}\int_0^\infty \langle F(t)\,F(t+T)\rangle\cos\omega T\,{\rm d}T, \\ g(\omega) &= \frac{2}{\pi}\int_0^\infty \langle x(t)\,x(t+T)\rangle\cos\omega T\,{\rm d}T, \end{aligned}\right\} \tag{7.21}$$

where the brackets denote ensemble averages. Note that

$$\langle F^2\rangle = \int_0^\infty f(\omega)\,{\rm d}\omega \quad \text{and} \quad \langle x^2\rangle = \int_0^\infty g(\omega)\,{\rm d}\omega.$$

If we now Fourier transform equation (7.20), we obtain $Z\tilde{x} = \tilde{F}$, where tildes denote Fourier components and the impedance

$$Z = \mu(-\omega^2 + {\rm i}\omega/\tau_{\rm c} + \Omega_{\rm b}^2). \tag{7.22}$$

Making use of the familiar result that

$$g(\omega) = f(\omega)/ZZ^*, \tag{7.23}$$

we have

$$\langle x^2\rangle = \int_0^\infty \frac{f(\omega)\,{\rm d}\omega}{ZZ^*}. \tag{7.24}$$

But since $1/\tau_{\rm c}$ (typically $\sim 10^{-4}$ a$^{-1}$ is much less than $\Omega_{\rm b}$ ($\gtrsim 1$ a$^{-1}$), equation (7.22) shows that $1/ZZ^*$ is nearly a delta function at the orbital frequency $\Omega_{\rm b}$, i.e. the damping is so weak that only forcing frequencies in a narrow window about the orbital resonance contribute. So to very good approximation,

$$\langle x^2\rangle = \tfrac{1}{2}f(\Omega_{\rm b})\,\pi\,\tau_{\rm c}/\mu^2\,\Omega_{\rm b}^2, \tag{7.25}$$

and so the average total orbital energy associated with the epicyclic motion

$$\langle E_e\rangle = \langle \tfrac{1}{2}\mu\Omega_{\rm b}^2\,x^2 + \tfrac{1}{2}\mu\dot{x}^2\rangle = \mu\Omega_{\rm b}^2\langle x^2\rangle = \tfrac{1}{2}\pi(\tau_{\rm c}/\mu)f(\Omega_{\rm b}). \tag{7.26}$$



PHILOSOPHICAL TRANSACTIONS OF THE ROYAL SOCIETY A MATHEMATICAL, PHYSICAL & ENGINEERING SCIENCES
PHILOSOPHICAL TRANSACTIONS OF THE ROYAL SOCIETY A MATHEMATICAL, PHYSICAL & ENGINEERING SCIENCES

Downloaded from rsta.royalsocietypublishing.org



Most of the power in the fluctuating force field will be at the eddy turnover frequency $\tau_{\rm eddy}^{-1}$ (equation (7.9)). At lower frequencies, the uncorrelated eddies should give a white noise spectrum. At higher frequencies the power spectrum of the fluctuating force falls as a steep power of frequency (the high frequency power is produced by the small density fluctuations of the Kolmogorov subeddies of the main convective eddies). The fall-off at high frequency is so rapid that to a good approximation, we may take

$$f(\omega) \simeq \begin{cases} \langle F^2 \rangle \tau_{\rm eddy}, & \omega < \tau_{\rm eddy}^{-1} = v_H H^{-1}; \\ 0 & \omega > \tau_{\rm eddy}^{-1}. \end{cases} \tag{7.27}$$

Using equation (7.19) and (7.17) to compute $\langle F^2 \rangle$, and inserting those in (7.27) and hence, with (7.8) into (7.26), we find that

$$\langle E_e \rangle \approx \rho H^3 v_H^2 / 4\pi \quad \text{or} \quad \Omega_{\rm b} < \tau_{\rm eddy}^{-1}; \tag{7.28}$$

i.e. the mean (ensemble or time average) energy in orbital epicyclic motion is just the energy in a single convection cell. As conjectured at the beginning of the subsection, this is completely analogous to $\langle E_{\rm pend} \rangle = kT_{\rm air}$ for a pendulum swinging in air. Equation (7.28) determines the mean square orbital eccentricity, since

$$E_e = \tfrac{1}{2} \mu \Omega_{\rm b}^2 a^2 e^2. \tag{7.29}$$

### (e) *Real giants and real pulsars*

To compute the mean square eccentricity of a binary system containing a real giant, we must sum the contributions to the power spectrum of the fluctuating force $f(\omega)$, just as we did in deriving the circularization time (7.11). Adopting the approximate spectrum (7.27), we find

$$\langle E_e \rangle = \sum_{\text{layers with } v_H/H > \Omega_{\rm b}} H^5 \rho^2 v_H^3 \Big/ \sum_{\text{all layers}} 4\pi \rho v_H H^2. \tag{7.30}$$

Eddy viscosity may be ineffective if $v_H/H < \Omega_{\rm b}$, in which case the sum in the denominator should also be restricted to $v_H/H > \Omega_{\rm b}$, which would modify (7.11) for very short period binaries (Zahn 1989). In the late stages of the evolution of a mass-transferring giant, the mass of the convective envelope is reduced to $M_{\rm env} \ll M_{\rm c}$ (see §4), and except in ionization zones, $p \propto \rho^{\frac{5}{3}}$. The equations of stellar structure then give

$$\rho = \rho_* (R_{\rm c}/r - 1)^{\frac{3}{2}}, \quad H = \tfrac{2}{3}(R_{\rm c} - r)\, r/R_{\rm c} \quad \text{and} \quad M_{\rm env} = \tfrac{1}{4}\pi^2 \rho_* R_{\rm c}^3,$$

and

$$v_H = \left(\frac{\pi L R_{\rm c}}{16 M_{\rm env}}\right)^{\frac{1}{3}} \left(\frac{r}{R_{\rm c} - r}\right)^{\frac{1}{2}} \left(\frac{R_{\rm c}}{r}\right)^{\frac{2}{3}}. \tag{7.31}$$

From the preceding, we see that the eddies have high frequencies at the surface and in the deep interior, but that at $r = \frac{7}{16} R_{\rm c}$, $v_H/H$ reaches a minimum $\min(v_H/H) \equiv 2\pi/P_{\rm crit}$. Thus in binaries with orbital periods $P_{\rm b}$ greater than

$$P_{\rm crit} \approx 2\pi \max_r (\tau_{\rm eddy}) \approx 25 (T_{\rm eff}/(7000\ {\rm K}))^{-\frac{4}{3}} (M_{\rm env}/(7 \times 10^{-3}\, M_\odot))^{\frac{1}{3}}\ {\rm d}, \tag{7.32}$$

all layers have frequencies above resonance, and so all contribute to the sum in the numerator of (7.30). In this case, if we insert the eddy properties of the simple

Downloaded from rsta.royalsocietypublishing.org



polytropic convective envelope described by equation (7.31) and the text preceding it into equation (7.30), we find

$$\langle E_e \rangle = \tfrac{1}{2}\mu\Omega_b^2 a^2 \langle e^2 \rangle = 3.4 \times 10^{-5} (L^2 R_c^2 M_{env})^{\frac{1}{3}}, \tag{7.33}$$

where the dimensionless prefactor comes from the dimensionless integrals over the density and convection velocity profiles in the envelope. Note that larger and more luminous giants, whose tenuous envelopes require more vigorous convection, have larger epicyclic energies, as might have been guessed from the simple single-layer equipartition result (7.28).

### (*f*) *Freeze-out and prediction of eccentricity*

While a neutron star's red giant companion is filling its Roche lobe, transferring mass and spinning up the neutron star, the orbit will have a mean square eccentricity given by (7.33). This eccentricity is a random variable, built up over the circularization time $\tau_c$ ($\sim 10^4$ years for a typical system) by the small fluctuating resonant forces (rapidly variable on a timescale $\sim H/v_H \lesssim 1$ year). From equation (7.20) and the white noise approximation (7.27), one can show that the eccentricity has decorrelation time $2\tau_c$:

$$\langle e(t)\, e(t+T) \rangle \propto \exp[-T/(2\tau_c)]. \tag{7.34}$$

By the time we see the spun-up neutron star as a radio pulsar, and measure the orbital eccentricities, however, its giant companion has become a white dwarf. Applying equation (7.33) to the white dwarf would predict an infinitesimal eccentricity. But the timescale $\tau_c$ (equation (7.11)) to reach that equilibrium would vastly exceed the age of the universe. So to determine the residual eccentricity of the pulsar-white dwarf binary, we must investigate more carefully what happens during the transition from a red giant to a white dwarf, as $\tau_c \to \infty$, and the eccentricity 'freezes out'. (The term 'freeze-out' is suggested by the very close analogy with reactions in an expanding universe. Neutrinos and neutrons, for example are initially in thermodynamic equilibrium. But as the universe expands, the reaction rates involving them become slower than the expansion rate, and their abundance becomes 'frozen'.) As mass transfer reduces the giant's envelope mass $M_{env}$ to about eight times the mass of the hydrogen burning shell ($\sim 10^{-3} M_\odot$) the radiative shell begins to react to the change in the hydrostatic pressure, and the giant's luminosity and radius begin to decrease (Refsdal & Weigert 1970, 1971; and §4). This contraction occurs on the nuclear timescale (from Refsdal & Weigert (1970) $\sim 10^7$ years for a $0.26 M_\odot$ giant filling the Roche lobe of a $P_b = 30$ d binary; $\sim 7 \times 10^5$ years for a $0.44 M_\odot$ giant filling the Roche lobe of a $P_b = 3$ years binary). This is initially much longer than $\tau_c$, so the orbital $\langle e^2 \rangle$ will be the equilibrium (7.33) appropriate to the shrinking envelope. But once $R \lesssim 0.5 R_{Lc}$ ($R_{Lc}$ is the radius of the giant's Roche lobe, $R_{Lc} \approx 0.25a$ for the binaries in the third group of table 3), the timescale for pumping and damping $e$, $\tau_c \propto R_c^{-8}$, becomes longer than the timescale on which the envelope is collapsing. The value of $e$ is then 'frozen' at the value it had when $R \approx 0.5 R_{Lc}$.

This gives us confidence that any pumping of the eccentricity by the accretion disc is irrelevant. After the dwindling giant has shrunk inside its Roche lobe, ending mass transfer and cutting off supply to the accretion disc, there are still hundreds of circularization times to erase the memory of any eccentricity excited by the accretion disc (or passing stars), and establish the equilibrium (7.33). Using, from Refsdal &



PHILOSOPHICAL TRANSACTIONS OF THE ROYAL SOCIETY A MATHEMATICAL, PHYSICAL & ENGINEERING SCIENCES
PHILOSOPHICAL TRANSACTIONS OF THE ROYAL SOCIETY A MATHEMATICAL, PHYSICAL & ENGINEERING SCIENCES

Downloaded from rsta.royalsocietypublishing.org



Weigert (1970), that at half maximum radius the 0.2–0.4$M_\odot$ shell burning giants have $M_{\rm env} \approx 7 \times 10^{-3} M_\odot$ and $T_{\rm eff} \approx 7000$ K in equation (7.33), we find that for the pulsar binaries

$$\langle e^2 \rangle^{\frac{1}{2}} \approx 1.5 \times 10^{-4} \, (P_{\rm b}/(100 \text{ d})) \quad \text{for} \quad P_{\rm b} > P_{\rm crit} \approx 25 \text{ d}. \tag{7.35}$$

The actual value of $e$ for a given binary pulsar cannot, of course, be predicted exactly, depending as it does on the random history of eddies around the time of freeze out. But the probability distribution $e^2$ at a given $P_{\rm b}$ is predicted to be nearly a Boltzmann distribution, $P(e^2)\,{\rm d}e^2 \propto \exp[-e^2/\langle e^2 \rangle]\,{\rm d}e^2$.

It is encouraging that the eccentricities of the pulsars with low mass white dwarf companions (third group in table 3) have eccentricities with numerical values of order those predicted by equation (7.35), and have the expected trend (mean square eccentricity increasing with orbital period; see discussion after (7.33)). The reader is referred to a forthcoming paper (Phinney 1992) for a more detailed derivation of these results, including higher multipoles than the quadrupole, Kolmogorov subeddies, behaviour for $P < P_{\rm crit}$, and integrations through realistic giant envelopes, including ionization zones. None of the complications considered lead to conclusions qualitatively (or even very quantitatively) different from the simple form of the theory presented here.

The foregoing is unusual among astrophysical theories in that it has no adjustable parameters; the eccentricity distribution as a function of $P_{\rm b}$ is predicted *a priori*. The modest success can be regarded either as inevitable (no one disbelieves that red giants are convective, nor that Newton's laws apply to orbits), or astonishing (convective turbulence is notoriously complicated, and one might have imagined that in rapidly rotating stars, there might have been dramatic correlations or severe anisotropy in the eddies). Large quadrupole moments could also be excited by Mira-type large amplitude non-radial pulsations for the extreme giants in long-period systems, and might be relevant to PSR0820+02.

## 8. Planets around pulsars

A planet of mass $m$ orbiting a pulsar of mass $M_{\rm p}$ in an orbit of semi-major axis $a$ and period $P_{\rm y}$ years produces a periodic timing residual of semiamplitude (cf. equation (1.5))

$$\frac{a_{\rm p} \sin i}{c} = \frac{m}{M_{\rm p}+m} \frac{a \sin i}{c} \approx 1700 \text{ μs} \frac{m}{M_\oplus} \left( \frac{1.4 M_\odot}{M_{\rm p}} \right)^{\frac{2}{3}} P_{\rm y}^{-\frac{2}{3}} \sin i. \tag{8.1}$$

Thus, for example in 1 year orbits around a $1.4 M_\odot$ neutron star, at $i = 60°$, Jupiter would produce a residual of semi-amplitude 0.46 s, Earth of 1.5 ms, the Moon of 18 μs, and the asteroid Ceres 0.3 μs. As discussed in §1, timing residuals of 1 μs can be measured for millisecond pulsars, so pulsar planetary systems containing anything bigger than Moon-size objects are potentially detectable. Some pulsars, e.g. PSR1937+21 (the original millisecond pulsar), clearly do not have any such planetary systems (Thorsett & Phillips 1992).

But after several false signals involving young pulsars with quasi-periodic timing noise and a millisecond pulsar whose incorrect position led a timing program to interpret a harmonic of the Earth's motion as a planet, there does now appear to be a millisecond pulsar, PSR1257+12, around which orbit not just one, but two planets. The system was discovered by Wolszczan & Frail (1992), and confirmed,



PHILOSOPHICAL TRANSACTIONS OF THE ROYAL SOCIETY A MATHEMATICAL, PHYSICAL & ENGINEERING SCIENCES
PHILOSOPHICAL TRANSACTIONS OF THE ROYAL SOCIETY A MATHEMATICAL, PHYSICAL & ENGINEERING SCIENCES

Downloaded from rsta.royalsocietypublishing.org



using an independent telescope, timing electronics, and Solar System ephemeris by Backer *et al.* (1992). The two planets are on nearly circular orbits of periods 67 and 98 days (table 3). Their mass functions suggest masses of a few times that of the Earth. If this interpretation is correct, it is amusing to note that the angular momentum in the neutron star spin $\sim 1.0 \times 10^{48}$ g cm$^2$ s$^{-1}$ (about a tenth the total angular momentum of the Sun!) is remarkably comparable with the total angular momentum of its two planets $\sim 1.4 \times 10^{48}$ g cm$^2$ s$^{-1}$. By contrast, Jupiter carries most of the angular momentum in the Solar System ($\sim 10^2$ times that of the Sun).

There have already been dozens of papers and a whole conference proceedings (Phillips *et al.* 1992) devoted to the problem of forming these planets. Thus I confine myself to a few general remarks. The planets cannot have been formed at the same time as the pulsar's progenitor (unless they perhaps were dragged in from very large radii, a process which appears very difficult to stop at the required final radii), since they would have been evaporated during the subsequent evolution. The pulsar has all the characteristics (short period, low magnetic field) of one recycled by accretion from a companion star, now vanished. This suggests that the planets may have formed from debris released in the disruption of its companion. The evolution of such a debris disc ought to be quite similar to that of the protosolar nebula, so it is perhaps not surprising that both led to planetary systems.

PSR1937+21 warns us, however, that either there is more than one way to disrupt a companion, or that not all debris discs form planetary systems. Despite these speculations, some sceptics are still worried by the possibility that the timing residuals are not caused by planets, but are a conspiracy of timing noise or pulsar precession. Fortunately, newtonian dynamics offers a promising way to test the planetary interpretation of PSR1257+12s residuals.

If the two planets lie in nearly the same orbital plane, as is expected if they formed from an accretion or excretion disc (cf. the Solar System), then for each choice of the inclination of the orbit to the line of sight (which determines the masses of the planets $\propto 1/\sin i$), one can make a definite prediction of the future orbits of the planets. First, one can rule out the (one in a million) possibility that the orbit is so precisely face-on that the masses of the planets are greater than that of Jupiter, for then numerical integrations show that their mutual interactions would be so great that one of them would have been ejected from the system long ago (Rasio *et al.* 1992).

Second, the planets are close to a 3:2 resonance: the inner planet goes around the pulsar $2.95 \approx 3$ times each time the outer one makes two revolutions in 196.4 d. Thus the relative configurations of the planets repeat almost exactly every $\sim 196.4$ d, so that their mutual gravitational effects on each others' orbits (e.g. their longitudes of periastron $\omega$ and orbital eccentricities $e$) can build up over many orbital periods. The difference of the planets' phases with respect to this near resonance changes with period $P_{\rm d}$ given by $1/P_{\rm d} = 2/P_{\rm in} - 3/P_{\rm out} = 1/(5.3 \text{ years})$, so that their $\omega$ and $e$ should vary almost periodically with period $P_{\rm d}$. The amplitude of the oscillations in $\omega$ and $e$ caused by these mutual interactions are of order 0.5–3% (Rasio *et al.* 1992) for $i \approx 60°$ (the median value), but scale linearly with the masses of the planets, i.e. as $1/\sin i$ for $\sin i \gtrsim 0.1$. For $\sin i \lesssim 0.1$, the masses of the planets are large enough that for some configurations, their mutual perturbations could cause their orbits to precess with a period of exactly $P_{\rm d}$, i.e. the planets could be locked in resonance. In this case (possible but *a priori* improbable) the phase and eccentricity variations can be even larger (Malhotra *et al.* 1992). Thus the existence of such variations in the planets' eccentricities and longitudes of periastron with a period of 5.3 years would

Downloaded from rsta.royalsocietypublishing.org



confirm that the phase oscillations are indeed planets, and (from the amplitude of oscillation) determine the orbital inclination.

## 9. Conclusion

It is striking what a broad range of newtonian dynamics pulsars allow us to explore, in ways no other objects have permitted. From mass-to-light ratios and mass segregation in globular clusters, to perturbation theory of the three-body problem, to the gravothermal catastrophe and chaos in the three- and four-body problem, to the fluctuating potentials of convective stars, to the dynamics of the first planetary system beyond our own. It is also striking that most of the pulsars which have allowed us to study these phenomena have been discovered in the past five years. If this pace of discovery continues until pulsars' golden anniversary, we may need to raise Sir Isaac from the grave to help us keep up with understanding it all.

The research described herein has been supported by NASA (grant NAGW-2394) and the Alfred P. Sloan Foundation. I thank J. Bahcall and P. Hut for their generous hospitality at the Institute for Advanced Study, were the initial draft was written. I thank N. Murray for allowing me to include his results in §5, and P. Goldreich and B. Paczynski for useful discussions of the material in §7. And I thank my collaborators S. Kulkarni, S. Sigurdsson and F. Verbunt for sharing three years of fun, insight and discovery.

## References

Numbers in parentheses at the end of a reference refer to those used in the tables.

Anderson, S., Kulkarni, S., Prince, T. & Wolszczan, A. 1990 *IAU Circ.* no. 5013. (13)

Anderson, S. B. & Prince, T. 1992 Personal communication. (3)

Anderson, S. B., Gorham, P. W., Kulkarni, S. R., Prince, T. A. & Wolszczan, A. 1990 *Nature, Lond.* **346**, 42–44. (1)

Artymowicz, P., Clarke, C. J., Lubow, S. H. & Pringle, J. E. 1991 The effect of an external disk on the orbital elements of a central binary. *Astrophys. J.* **370**, L35–L38.

Aurière, M. & Koch-Miramond, L. 1991 X1850-086. *IAU Circ.* no. 5364.

Backer, D., Sallmen, S. & Foster, R. 1992 Pulsar's double period confirmed. *Nature, Lond.* **358**, 24–25.

Biggs, J. D., Lyne, A. G., Manchester, R. N. & Ashworth, M. 1990 *IAU Cir.* no. 4988 (4).

Blandford, R. D., Narayan, R. & Romani, R. W. 1984 Arrival-time analysis for a millisecond pulsar. *J. Astrophys. Astr.* **5**, 369–388.

Blandford, R. D., Romani, R. W. & Applegate, J. H. 1987 Timing a millisecond pulsar in a globular cluster. *Mon. Not. R. astr. Soc.* **225**, 51*P*–53*P*.

D'Amico, N., Lyne, A. G., Bailes, M., Johnston, S., Manchester, R. N., Stavely-Smith, L., Lim, J., Fruchter, A. S. & Goss, W. M. 1990 *IAU Cir.* no. 5013. (11)

Deich, W. 1992 Personal communication. (16)

Fabian, A. C., Pringle, J. E. & Rees, M. J. 1975 Tidal capture formation of binary systems and X-ray sources in globular clusters. *Mon. Not. R. astr. Soc.* **172**, 15*P*–18*P*.

Fahlman, G. G., Richer, H. B. & VandenBerg, D. A. 1985 Deep CCD photometry in globular clusters. III. M15. *Astrophys. J. Suppl. Ser.* **58**, 225–254.

Foster, R. S., Backer, D. C. & Taylor, J. H. 1988 *Astrophys. J.* **326**, L13–L15. (7)

Gao, B., Goodman, J., Cohn, H. & Murphy, B. W. 1991 Fokker–Planck calculations of star-clusters with primordial binaries. *Astrophys. J.* **370**, 567–582.

Griffin, R. F. 1991 Spectroscopic binary orbits from photoelectric radial-velocities – a synopsis of papers 1–100. *Observatory* **111**, 291–298.

Gunn, J. E. & Griffin, R. F. 1979 Dynamical studies of globular clusters based on photoelectric radial velocities of individual stars I:M3. *Astr. J.* **84**, 752–773.



PHILOSOPHICAL TRANSACTIONS OF THE ROYAL SOCIETY A MATHEMATICAL, PHYSICAL & ENGINEERING SCIENCES

PHILOSOPHICAL TRANSACTIONS OF THE ROYAL SOCIETY A MATHEMATICAL, PHYSICAL & ENGINEERING SCIENCES

Downloaded from rsta.royalsocietypublishing.org



Heggie, D. C. 1975 Binary evolution in stellar dynamics. *Mon. Not. R. astr. Soc.* **173**, 729–787.

Heggie, D. C. & Aarseth, S. J. 1992 Dynamical effects of primordial binaries in star clusters, I. Equal masses. *Mon. Not. R. astr. Soc.* **257**, 513–536.

Hills, J. G. 1976 The formation of binaries containing black holes by the exchange of companions and the X-ray sources in globular clusters. *Mon. Not. R. astr. Soc.* **175**, 1*P*–4*P*.

Hjellming, M. S. & Webbink, R. F. 1987 Thresholds for rapid mass-transfer in binary systems. 1. Polytropic models. *Astrophys. J.* **318**, 794–808.

Hut, P. 1983 Binaries as a heat source in stellar dynamics: release of binding energy. *Astrophys. J.* **272**, L29–L33.

Johnston, H. M., Kulkarni, S. R. & Phinney, E. S. 1992 Statistics of pulsars in globular clusters. In *Neutron stars in binary systems* (ed. E. van den Heuvel & S. Rappaport). (In the press.)

Johnston, S., Manchester, R. N., Lyne, A. G., Bailes, M., Kaspi, V. M., Guojun, Q. & D'Amico, N. 1992 *Astrophys. J.* **387**, L37–L41. (17)

Jones, A. W. & Lyne, A. G. 1988 *Mon. Not. R. astr. Soc.* **232**, 473–480. (Note that $f(M)$ is incorrectly stated in this reference.) (22)

Joss, P. C., Rappaport, S. & Lewis, W. 1987 The core mass-radius relation for giants: a new test of stellar evolution theory. *Astrophys. J.* **319**, 180–187.

King, E. S. 1920 Standard velocity curves for spectroscopic binaries. *A. Harvard Obs.* **81**, 231.

Krolik, J. H., Meiksin, A. & Joss, P. C. 1984 The evolution of highly compact binary stellar systems in globular clusters. *Astrophys. J.* **282**, 466–480.

Kulkarni, S. R. 1992 Personal communication. (15)

Kulkarni, S. R., Anderson, S. B., Prince, T. A. & Wolszczan, A. 1991 *Nature, Lond.* **349**, 47–49. (14)

Kulkarni, S. R., Goss, W. M., Wolszczan, A. & Middleditch, J. 1990 Deep radio synthesis images of globular clusters. *Astrophys. J.* **363**, L5–L8.

Lauer, T. R. *et al.* 1991 The postcollapse core of M15 imaged with the HST planetary camera. *Astrophys. J.* **369**, L45–L49.

Lyne, A. G. 1984 Orbital inclination and mass of the binary pulsar PSR0655+64. *Nature, Lond.* **310**, 300–302.

Lyne, A. G. & Bailes, M. 1990 *Mon. Not. R. astr. Soc.* **246**, 15*P*–17*P*. (21)

Lyne, A. G. & McKenna, J. 1989 *Nature, Lond.* **340**, 367–369. (18)

Malhotra, R., Black, D., Eck, A. & Jackson, A. 1992 Resonant orbital evolution in the putative planetary system of PSR1257+12. *Nature, Lond.* **356**, 583–585.

Manchester, R. N., Lyne, A. G., D'Amico, N., Johnston, S., Lim, J. & Kniffen, D. A. 1990 *Nature, Lond.* **345**, 598–600. (8)

Manchester, R. N., Lyne, A. G., Johnston, S., D'Amico, N., Lim, J., Kniffen, D. A., Fruchter, A. S. & Goss, W. M. 1989 *IAU Cir.* no. 4905. (5)

Manchester, R. N., Lyne, A. G., Robinson, C., D'Amico, N., Bailes, M. & Lim, J. 1991 *Nature, Lond.* **352**, 219–221. (9)

Massey, P. & Thompson, A. B. 1991 Massive stars in Cyg OB2. *Astr. J.* **101**, 1408–1428.

McKenna, J. & Lyne, A. G. 1988 *Nature, Lond.* **336**, 226–227. (12)

McMillan, S. L. W., McDermott, P. N. & Taam, R. E. 1987 Formation and evolution of tidal binary systems. *Astrophys. J.* **318**, 261–277.

Meylan, G., Dubath, P. & Mayor, M. 1991 Core velocity dispersion in high concentration globular clusters. *Bull. Am. astr. Soc.* **23**, 833–834.

Murphy, B. W., Cohn, H. N. & Hut, P. 1990 Realistic models for evolving globular clusters II. Post core collapse with a mass spectrum. *Mon. Not. R. astr. Soc.* **245**, 335–349.

Naylor, T., Charles, P. A., Drew, J. E. & Hassall, B. J. M. 1988 Spectroscopy of the M15 X-ray sources: discovery of binary motion and an unusual systemic velocity. *Mon. Not. R. astr. Soc.* **233**, 285–304.

Pan, X. P., Shao, M., Colavita, M. M., Armstrong, J. T. & Mozurkewich, D. 1992 Determination of the visual orbit of the spectroscopic binary $\alpha$ Andromedae with submilliarcsecond precision. *Astrophys. J.* **384**, 624–633.



PHILOSOPHICAL TRANSACTIONS OF THE ROYAL SOCIETY A MATHEMATICAL, PHYSICAL & ENGINEERING SCIENCES

PHILOSOPHICAL TRANSACTIONS OF THE ROYAL SOCIETY A MATHEMATICAL, PHYSICAL & ENGINEERING SCIENCES

Downloaded from rsta.royalsocietypublishing.org



Peterson, R. C., Seitzer, P. & Cudworth, K. M. 1989 The nonthermal stellar dynamics of the globular cluster M15. *Astrophys. J.* **347**, 251–265.

Phillips, J. A., Thorsett, S. E. & Kulkarni, S. R. (eds) 1992 *Planets around pulsars*. San Francisco: Astronomy Society Pacific. (In the press.)

Phinney, E. S. & Sigurdsson, S. 1991 Ejection of pulsars and binaries to the outskirts of globular clusters. *Nature, Lond.* **349**, 220–223.

Phinney, E. S. & Verbunt, F. 1991 Binary pulsars before spin-up and PSR 1820–11. *Mon. Not. R. astr. Soc.* **248**, 21P–23P.

Phinney, E. S. 1992 Accelerations and relaxation of pulsars in globular clusters. *Mon. Not. R. astr. Soc.* (In the press.)

Predehl, P., Hasinger, G. & Verbunt, F. 1991 Rosat discovery of bright X-ray sources in globular clusters Ter6 and NGC6652. *Astr. Astrophys.* **246**, L21–L23.

Prince, T. A., Anderson, S. B., Kulkarni, S. R. & Wolszczan, A. 1991 *Astrophys. J. Lett.* **374**, L41–L44. (2)

Pryor, C., McClure, R. D., Hesser, J. E. & Fletcher, J. M. 1989 Frequency of primordial binary stars in globular clusters. In *Dynamics of dense stellar systems* (ed. D. Merritt), pp. 175–181. Cambridge University Press.

Rappaport, S., Putney, A. & Verbunt, F. 1989 Evolution of wide binary millisecond pulsars in globular clusters. *Astrophys. J.* **345**, 210–221.

Rasio, F. A., Nicholson, P. D., Shapiro, S. L. & Teukolsky, S. A. 1992 An observational test for the existence of a planetary system orbiting PSR1257 + 12. *Nature, Lond.* **355**, 325–326.

Rawley, L. A., Taylor, J. H. & Davis, M. M. 1988 *Astrophys. J.* **326**, 947–953. (24)

Refsdal, S. & Weigert, A. 1970 Shell source burning stars with highly condensed cores. *Astr. Astrophys.* **6**, 426–440.

Refsdal, S. & Weigert, A. 1971 On the production of white dwarfs in binary systems of small mass. *Astr. Astrophys.* **13**, 367–373.

Ryba, M. F. & Taylor, J. H. 1991 *Astrophys. J.* **371**, 739–748. (26)

Ryba, M. F. & Taylor, J. H. 1991 *Astrophys. J.* **380**, 557–563. (27)

Sigurdsson, S. 1991 Dynamics of neutron stars and binaries in globular clusters. Ph.D. thesis, California Institute of Technology.

Sweigart, A. V. & Gross, P. G. 1978 Evolutionary sequences for red giant stars. *Astrophys. J. Suppl. Ser.* **36**, 405–437.

Taylor, J. H. 1992 Personal communication. (25)

Taylor, J. H. & Dewey, R. J. 1988 *Astrophys. J.* **332**, 770–776. (23)

Taylor, J. H. & Weisberg, J. M. 1989 *Astrophys. J.* **345**, 434–450. (19)

Thorsett, S. E. & Nice, D. J. 1991 *Nature, Lond.* **353**, 731–733. (6)

Thorsett, S. E. & Phillips, J. A. 1992 Rocks around the clock: limits on pulsar planetary systems. *Astrophys. J.* **387**, L69–L71 (29).

Van Paradijs, J. 1983 Optical observations of compact galactic X-ray sources. In *Accretion-driven stellar X-ray sources* (ed. W. H. G. Lewin & E. P. J. van den Heuvel), pp. 189–260. Cambridge University Press.

Verbunt, F., van den Heuvel, E. P. J., Van Paradijs, J. & Rappaport, S. A. 1987 Formation of isolated millisecond pulsars in globular-clusters. *Nature, Lond.* **329**, 312–314.

Wolszczan, A. 1991 *Nature, Lond.* **350**, 688–690. (20)

Wolszczan, A. & Frail, D. A. 1992 A planetary system around the millisecond pulsar PSR1257 + 12. *Nature, Lond.* **355**, 145–147. (28)

Wolszczan, A., Anderson, S. B., Kulkarni, S. R. & Prince, T. A. 1989 *IAU Cir.* no. 4880. (10)

Zahn, J.-P. 1966 Les marées dans une étoile double serrée. *Annales d'Astrophysique* **29**, 313–330; 489–506; 565–591.

Zahn, J.-P. 1977 Tidal friction in close binary stars. *Astr. Astrophys.* **57**, 383–394; Erratum **67**, 162.

Zahn, J.-P. 1989 Tidal evolution of close binary stars revisited. *Astr. Astrophys.* **220**, 112–116.



PHILOSOPHICAL TRANSACTIONS OF THE ROYAL SOCIETY A MATHEMATICAL, PHYSICAL & ENGINEERING SCIENCES

PHILOSOPHICAL TRANSACTIONS OF THE ROYAL SOCIETY A MATHEMATICAL, PHYSICAL & ENGINEERING SCIENCES